1974

An experimental approach to the problem of a near-wake in pulsating flows with axial pressure gradients /

Ferruccio Pittaluga
Lehigh University

AN EXPERIMENTAL APPROACH TO THE PROBLEM OF A NEAR-WAKE IN PULSATING FLOWS WITH AXIAL PRESSURE GRADIENTS

by

Ferruccio Pittaluga

A Thesis

Presented to the Graduate Committee

of Lehigh University

in Candidacy for the Degree of

Master of Science

in

Mechanical Engineering

Lehigh University

1974

This thesis is accepted and approved in partial fulfillment of the requirements for the degree of Master of Science

Sept 18, 1974
(date)

Donald Rockwell
Professor in Charge

Robert A. Laudise for PPB
Chairman of Department

ACKNOWLEDGEMENTS

A sincere, thankful acknowledgement is due to my advisor, Dr. D.O. Rockwell, not only for the most valuable guidance he gave to me throughout the present work, but also for his encouraging support whenever difficulties arose. I am also grateful to Professor F.T. Brown and Professor S. Johnson who made possible the use of the computer for this research.

Finally, I am indebted towards all the technicians of the M.E. Dept. in Lehigh for being always kindly available in building and repairing the whole equipment.

TABLE OF CONTENTS

LIST OF TABLES AND FIGURES

NOMENCLATURE AND DEFINITIONS

Symbols:

d	Wake generator diameter
D	Diffuser diameter
L	Diffuser length
p	Pressure
R	Diffuser radius
t	Time
T	Period
u	Velocity component in x-direction
x	Axial coordinate
y	Radial coordinate
ϕ	Phase angle
ρ	Density
ν	Kinematic viscosity
ω	Radian frequency

Indices:

i	Diffuser inlet

Special Notations:

$\overline{f}$	Time average of f
$\|f\|$	Peak-to-peak oscillation amplitude of f

Definitions:

$A_r = \frac{\lvert u \rvert}{\lvert u_i \rvert}$	Amplitude ratio
$Re_d = \frac{\bar{u}_i d}{\nu}$	Sphere Reynolds number
$Re_D = \frac{\bar{u}_i D_i}{\nu}$	Diffuser Reynolds number
$St_d = \frac{\omega d}{\bar{u}_i}$	Sphere Stouhal number
$St_D = \frac{\omega D_i}{\bar{u}_i}$	Diffuser Strouhal number
T-1, 2, 3, 4, 5	Oscillation periods defined in paragraph 3.
X-1, 2, 3, 4, 5	Diffuser axial locations defined in paragraph 3.

ABSTRACT

A hot-wire anemometer study of a turbulent near-wake in oscillating flows within two conical diffusers is presented. Time-mean velocity and turbulence intensity traverses are given, together with organized wave amplitudes and phases evaluated at the most significant points in the flow field by means of an ensemble average technique. The Reynolds number based on the diffuser inlet diameter was about 4×10^4. The frequency of the superposed oscillations was varied from about 9 to about 140 cps. For the lower frequencies it was found that the oscillation amplitudes in the near-wake were always smaller than in the free-stream. At higher frequencies the oscillations showed amplitude peaks well above the free-stream values, but rapidly decaying with axial distance. The location of the peaks suggested that their origin might be traced to oscillation amplifications taking place in the wake generator boundary layer. Intermediate frequency oscillations decayed at the lowest rate in both diffusers.

1. INTRODUCTION

1.1. Previous Investigations

Of particular importance in the field of unsteady flows are the oscillatory phenomena induced in wall boundary layers and free shear layers by periodic disturbances acting in the free stream flow. With reference to boundary layers, the possibility of amplifications, relative to the free stream oscillation amplitudes, has been proved experimentally and theoretically, for both laminar and turbulent flows, by several authors; Hill and Stenning [2] , McDonald and Shamroth[5], Karlsson [3] , and others. Most recently, a study carried out at Lehigh University by Schachenmann [6] has shown the critical importance of a positive pressure gradient in magnifying perturbations in the boundary layers of long diffusers. To our knowledge, however, no data are available dealing with the behavior of wakes in oscillating flows - a problem which is important in understanding turbomachinery performance, since the turbine or compressor rotor blades rotate through the near-wakes of the stator vanes located upstream. Marine propellers and helicopter rotors are other examples in which a better knowledge of pulsating wakes is of fundamental importance.

The fact that prevents an easy insight into a wake, particularly a near-wake, is its intrinsic highly fluctuating character, even in a steady free stream situation, with a closely related three-dimensionality of the velocity field. Nevertheless, it would be extremely

interesting to know if periodic free-stream disturbances are either completely washed out in the randomness of the wake flow or, conversely, at least in some frequency range, if they are still felt in an "average" sense as statistically organized disturbances. If the latter situation occurs, the next step would be to evaluate how the disturbances behave and if they can be enhanced in particular conditions. The present effort seeks the above objectives, as now it will be pointed out.

1.2. Preliminary Investigations and Objectives of the Thesis

The first aim of the present work was rather general, namely to check if harmonic oscillations superposed on a mean steady flow could produce variations in mean flow parameters, particularly in the shapes of the boundary layers and in the time mean velocity profiles. To this end, velocities and turbulence intensities were measured at several axial locations in two conical diffusers, one of 6^{o}, the other of 10^{o} total included angles. Horizontal and vertical traverses were performed and the results recorded. Although the rms readings varied sensibly with the frequency of the superposed oscillations, no detectable variations in time mean parameters were shown. This result is in line with reference [6] .

At this point a wake was generated at the inlet of each of the diffusers, again detecting no sensible frequency-related effect on the time mean flows. However, interesting phenomena were detected with regard to the turbulence intensities, which showed clear peaks at

particular stations within the diffusers when selected frequencies were being applied. Because of the highly turbulent signals we could not, using the oscilloscope, state if those peaks were originated by an increase in the organized oscillation amplitudes or by higher random fluctuation contribution. It was then decided to get a better insight into the above phenomena using a computer capable of analyzing the turbulent signals from the hot-wire by means of a recurrent sampling technique, which enabled extraction of the harmonic components from the turbulent background.

The following data were taken:

1) Complete maps of time mean velocity, rms of turbulent velocity fluctuations, oscillation amplitudes and phases at seven axial stations in the 10^{o} total included angle diffuser. This diffuser was 12 in. long and had a wake generator at its inlet. At an inlet Reynolds number $Re_D = 40,000$, the applied oscillation frequencies were in the low-medium range ($0.25 \leq St_D \leq 1.7$).

2) Centerline turbulence intensity and boundary layer oscillation amplitude measurements at chosen stations in the said diffuser for several Reynolds numbers, the highest being $Re_D = 70,000$. Corresponding oscillation frequencies were in the low-medium frequency range ($0.2 \leq St_D \leq 1.5$).

3) Complete maps of time mean velocity, rms values, oscillation amplitudes and phases in the near-wake regions of the 6^{o} and the

10^{o} total included angle diffusers, at $Re_D = 40,000$, with superposed frequencies ranging from low to very high values ($0.235 \leq St_D \leq 3.904$).

From 1) and 2) it was definitely ascertained that localized oscillation amplifications, in place of the expected oscillation decay with axial distance from inlet, can occur along the centerline of conical diffusers, even in the turbulent regime, with and without wakes at the inlet. These amplifications were accompanied by a double-frequency oscillating boundary layer at the locations where they took place. This important result is to be compared with that which is presented in reference [8] , the latter dealing only with diffusers in the laminar transitional regime. However, to avoid presenting data so far not completely organized in a comprehensive manner, only the results from above listed part 3) will be discussed herein. The other parts will be published separately. The description of part 3) concerning the mechanics of the oscillations in the near-wake represents the first study of this phenomenon.

2. MEASUREMENTS

2.1. Description of the Experimental Apparatus

A small wind tunnel with the capability of generating oscillatory flow was assembled. Its dimensions are shown in figure 1. The air was supplied from the laboratory compressed air circuit through a pressure regulator which kept the pressure upstream of the flow

regulating valve constant. The air then was fed into a stagnation tank followed by a rotating valve that generated the oscillation superposed on the mean flow. Downstream of this valve, the flow passed through another stagnation tank, particularly designed to damp out any flow asymmetries caused by the valve: to this end, it was rather long, with two separate honey-combs and three wire screens. The flow was then accelerated in a nozzle and passed through a section of straight pipe into the diffuser. A wake was generated by a sphere located on the centerline at the inlet of the diffuser. The sphere was supported by two vertical accurately tightened wires. The supported sphere system exhibited insignificant vibration. At the exit of the diffuser the air was discharged into the laboratory.

A detailed description of each of the important components is given below:

1) Air Compressors

- Worthington Reciprocating Compr. 6/6/5 x 5

Model HD8 - 6 cyl. - Air cooled

- Ingersoll Rand Reciprocating Compr. 7 x 7 1 cyl - water cooled

2) Compressed Air Dryer

Dynamic Dehumidifier - Pall Trinity Micro Corp. - Cortland - N.Y. Model: Trin. Cor. 3901 - Heat - Les

This instrument proved extremely important, as it will be pointed out later in connection with the hot-wire anemometer performance.

3) Pressure Regulator

Moore Products Co. Model 42H50 - Nullmatic

4) Stagnation Tanks

Plexiglass tube 6 in. diameter

5) Oscillating Valve

A schematic of the valve is shown in figure 2. A rectangular plate rotates in front of a fixed plate with two openings for the through flow and two vent openings. The vents open when the through flow is obstructed by the valve plate and therefore prevent a buildup of pressure in the upstream stagnation tank. This pressure buildup causes a severe distortion of the sine wave signal if the vents are blocked. The amplitude of the oscillation can be controlled by displacing the rotating plate with respect to the fixed one. Owing to this variable gap between the two plates, it would have been possible to adjust the oscillation amplitude almost independently from the frequency. However, due to the necessity of dismantling some connections each time an adjustment would be required, no independent amplitude settings were performed in the present research. The valve is driven by variable speed motor and control: Minarik Electric Co. - Model SH-32 with Bodine Electric D. C. Motor. Various belt drive arrangements were required to cover the range from low to high frequencies. The design of the valve gives velocity fluctuations that are nearly pure sinusoids. A sample oscillo-

scope trace is shown in figure 2 for the time dependent core velocity ahead of the sphere. Even in the highly turbulent region downstream of the sphere (near-wake) the trace on the computer-controlled scope readout recovered an almost perfect sine wave for each frequency after the phase averaging process, which will be discussed later.

6) Flow Straighteners

The straighteners are honeycombs made of aluminum foil. The cells are hexagonal, 1/8 in. diameter.

7) Wire Screens

Standard wire screens, 20 mesh, 0.016 in. wire diameter, 46.2% open area.

8) Nozzle

The nozzle contour is a circular arc. The nozzle exit diameter is 2.0 in., the area ratio is 9:1.

9) Wake Generator

The wake is generated by an alloy-steel sphere of an undamaged ball-bearing. The diameter is 0.31 in. and the surface is polished. Accurate cleaning was performed. The sphere is held in position right at the centerline of the diffuser inlet, by two vertical guitar wires glued on the sphere surface with a very small amount of epoxy glue and clasped, at the other end, inside the joint between the diffuser and the upstream cylindrical tube. The dimensions of the two glue drops on the sphere surface are of the same order of magnitude as the

wire diameter. The diameter of the wires is 0.009 in. The wires are vertical and straight. Their short length, together with the firm mounting, prevent any vibrations of themselves and of the sphere.

10) Diffusers

Both diffusers are conical, 12 in. long, and made of fiberglass and epoxy resin. One has an opening angle of 6^{o} (half opening angle 3^{o}), inlet diameter 2 in. and an outlet diameter of 3.28 in. The other diffuser has an opening angle of 10^{o} (half opening angle 5^{o}), inlet diameter 2 in. and an outlet diameter of 4.1 in. In the present study only the first 3 in. of each diffuser length (near-wake regions) have been investigated. Pressure taps are provided throughout the length of the diffusers at intervals of 1.5 in. A constant diameter tube 3.5 in. long was inserted between the nozzle exit and the diffuser inlet, mainly to get a detectable turbulent boundary layer thickness at the diffuser inlet and to avoid interference between the nozzle and the wake generator.

2.2. Instrumentation

2.2.1. Velocity Measurements

The air velocity was measured using a DISA hot-wire anemometer system, consisting of the following components.

DISA 55 A 25 Hot wire probes (straight)

DISA 55 D 01 Hot wire anemometer

DISA 55 D 10 Linearizer

DISA 55 D 30 DC Voltmeters (2)

DISA 55 D 35 RMS Voltmeter (Integrator)

The system was calibrated using the standard procedures recommended by DISA.

A traversing mechanism was used that enables the hot wire probes to be positioned horizontally, vertically and longitudinally within the diffuser. The horizontal and vertical traversing gears are connected to position transducers of the potentiometer type whose signals are fed, independently, into the x-input of a Hewlett-Packard Model 7035 B x-y Recorder, the y-input being either the actual velocity signal directly from the linearizer or the rms reading from the integrator.

2.2.2. Pressure Measurements

1) Time Mean Pressure

Time mean pressures were measured using a Flow Corporation (Cambridge-Mass) Micromanometer - Model MM3 containing Butyl.

2) Time Mean Pressure Difference

For pressure differences (mainly dynamic pressures) a Statham Model PL 283 TC-0.3-350 Pressure Transducer with a Statham Strain Gage Signal Amplifier Model CA 17-0-14741 were used. No negative dynamic pressures were detected even in the first traverse right behind the sphere.

3) Probes

The probes used to measure static and dynamic pressures had diameters of .094" and holes of .031". No detectable static pressure variations were encountered during a complete traverse at each axial location.

2.2.3. Oscillation Frequency

The frequency of oscillation of the valve which produced the unsteady flow was determined with a photocell circuit. The rotating plate interrupted the light path between a bulb and a photocell, resulting in a square wave signal with the frequency of the superposed flow oscillations. The frequency of the signal was measured with a Hewlett-Packard 5216A electronic counter. This same circuit was also used to provide a trigger signal for the timing of the oscillatory data evaluation.

2.2.4. Oscillatory Data Evaluation

1) Computer

For oscillatory data evaluation, a DEC LAB 8/E computer system was available. It consists of:

PDP 8/e	12 bit digital computer
AD8 -EA	A/D Converter
AM8 - EA	Multiplexer
2 DEC TAPE	Magnetic tape handlers
33 ASR	Teletype and paper tape reader/punch
VC8-E	Display control

2) Zero Suppressor

The A/D Converter-Multiplexer input was limited to signals of ± 1V. It was therefore necessary to condition the signals as follows: The dc component of the signals had to be taken out while all ac signal components passed through unchanged. This was accomplished using the electronic circuit shown in figure 3. The circuit uses two cascaded operational amplifiers MC 1741. Potentiometer R5 is used to offset the dc level of the input signal. The maximum range of R5 is ± 15 V. The gain of the whole circuit is nominally unity, but it can be fine tuned using trim potentiometer R7. The bandwidth of the circuit is dc to 10 kHZ.

2.3. Measurement Procedures

The steady flow field (no applied oscillations) in the diffusers was measured at the same value of the Reynolds number used in the measurement of the unsteady flow field (with oscillations) in order to have a basis for comparison. This is valid separately for each diffuser, whereas the Reynolds number for the 6^{o} angle diffuser was slightly higher than the one for the 10^{o} angle diffuser. The configuration for all the measurements was always with the sphere at the diffuser inlet. Careful and lengthy checks for axisymmetry were performed, each time a series of measurements were made. Horizontal

and vertical traverses at the same axial location were performed to ascertain symmetry at chosen axial locations.

The x-y recorder was used to record:

1) Velocity traverses from the linearized hot-wire signal.

2) Pressure traverses from the pressure transducer.

3) Traverses of the root-mean-square of the integral turbulence from the integrator.

The computer was used to extract, via ensemble averaging, amplitude and phase of the organized velocity oscillations at given locations within the diffusers. For purposes of comparison, these locations were at the same axial stations where above mentioned velocity and rms traverses were taken. The signal flow in the measuring system is shown in figure 4. The hot wire velocity signal is linearized and fed into the zero-suppressor circuit which removes the mean component of the velocity itself. The signal is then displayed on an oscilloscope. Use of the dc mode allows a check to be made of the dc level of the signal and makes it possible to adjust the zero suppressor. At the same time a check that the extreme values of the signal do not exceed the A/D converter input limit of ± 1 Volt can be made. If this is not the case, adjustment of the linearizer gain must be performed. This was particularly necessary for the points in the near-wake very close to the sphere. The signal then passes through the A/D converter to the computer input. The computer, using the timing signal provided

by the photocell trigger circuit, processes the signal and outputs the ensemble average of the velocity signal on the teletype.

Prior to each series of measurements, the following checks were made:

1) Sphere position and symmetry of flow.

2) Hot-wire system calibration,which was always found excellent with no detectable drift. This has been attributed to the cleanliness of the air as a result of passing through a dynamic de-humidifier downstream of the compressors. Nevertheless, frequent re-calibrations were performed following DISA instructions.

3) Free-stream Reynolds number at the diffuser inlet.

4) Air and room temperature.

Throughout the present study, with the exception of the computer and oscilloscope, all the electronic instruments were never turned off but switched to stand-by when not operating.

2.4. Data Processing

The ensemble averager program is part of the software package of the LAB 8/e system. It is described in detail in the LAB 8/e Software System User's Manual [9] . The program digitizes analog inputs and takes ensemble averages of these signals. A schematic of the sampling technique is shown in figure 5. The program samples the data at regular time intervals specified by the user. The start of the sampling is given by the trigger signal. After a specified number

of data points has been sampled, the sampling stops, and the program does the necessary calculations. As soon as the next trigger impulse is received, the program starts sampling again. The number of sweeps of sampling can be specified. After sampling is completed in all its sweeps, the program displays the average of the data taken on the oscilloscope screen. If the quality of the averages is not satisfactory, an additional number of sweeps can be added. When the data taking is finished, the program does a statistical evaluation of the sampled data. Calculation of a 95% confidence limit and of the signal trend can be done. The program then outputs data and statistics on the teletype and/or papertape.

2.5. Error Considerations and Data Qualification

Throughout the present work the precision of the experimental results was limited due to the reasons which follow. It is our feeling that the order of listing reflects also an expected order of importance.

1) Number of Data Points Available

With reference to the oscillation measurements, the time required to evaluate one data location in the flow field was rather long. The time ranged from 20 to 40 minutes, respectively, for very low frequencies and turbulence levels and very high ones, because the sweep intervals and the number of sweeps performed by the computer had to increase accordingly. For this reason, particularly in regions of high gradients of oscillation amplitude, the continuous lines in our

figures connecting the data points are not as accurate as they would if more points were available. On the other hand, the selection of the location of the points was many times aided by relatively quick checks on the computer scope, prior to performing the necessary sweeps.

2) Relative Size of the Hot-Wire Probe and Three-Dimensionality of the Flow

The presented results are in actuality not "local" but rather averaged over a region of the order of magnitude of the hot-wire length. Moreover, in the near-wake, only the apparent longitudinal components of the actual three-dimensional oscillating flow field have been measured.

3) Asymmetries of Flow and Influence of the Wake Generator Supports

The wires supporting the sphere at the diffuser inlet generated two wakes in a vertical plane which were felt both in the mean velocity and in the rms vertical traverses. The average free stream velocity in a vertical traverse (through the centerline of the diffuser) was about 8% lower than in a horizontal traverse. The rms readings during vertical traverses with superposed oscillations were, on the average, about 5% higher than in the horizontal plane, with reference to the free stream. A few checks of the oscillation amplitudes performed, at a fixed axial location, in points symmetrically located on the left and right hand side in a horizontal plane, as well as on the upper and lower part in a vertical plane, did not show any systematic difference. All

the results shown in our figures come from data points taken in horizontal planes.

4) Traversing Equipment Accuracy, Misalignment of the Probe, Vibrations

We estimate in $\pm$ 4% the total error due to these causes. The precision of the probe positioning was within $\pm$ 0.03".

5) Computer Results - Overall Accuracy

a) The zero suppressor was calibrated to give a gain of 1 $\pm$ 2%. The uncertainty is caused by a slight dependence of the gain on the operating temperature of the instrument. The frequency response of the suppressor circuit was checked and found to be flat from dc to 10 kHZ. The A/D converter and multiplexer accuracy is $\pm$ .1% of the maximum input signal value ($\pm$ 1V) and the frequency response is flat up to 30 kHZ. All input and output impedances of the components in the signal processing circuit were matched properly.

b) The averager program evaluated 95% confidence limits of the averaged value. The number of sweeps was selected to give, even in the highest turbulence intensities (e.g. just downstream of the sphere), an accuracy of $\pm$ 3% of the calculated oscillation amplitude. To this end, generally speaking, 500 sweeps were required for the free stream flow and up to 2500 sweeps in the first stations behind the sphere. The signal, averaged by the computer and displayed on the scope, was generally sinusoidal throughout the free stream and the

wake flow, with deformations, in the latter case, due to higher harmonics, of minor importance as far as the amplitude is concerned. On the other hand, effects of higher harmonics, constancy of the oscillation frequency of the valve ($\pm$ 1%), trigger rise time (.1 m sec at 35 HZ), and number of points per cycle displayed on the scope and printed (between 60 and 40), all contributed to an accuracy of no more than $\pm 10^{o}$ for the phase evaluation at the highest frequencies and of $\pm 6^{o}$ for the low-medium frequencies. No Fourier analysis was done on the computer results.

6) Hot-Wire Anemometer And Linearizer

All the DISA Instructions For Calibration were carefully followed. Almost no drift was detected. The calibration was done against a pitot static probe in steady flow, with no wake generator, at the diffuser centerline. The flow velocity was determined from the pressure difference across the pitot static tube using Bernoulli's equation. The uncertainty for the velocity, taking also into account the accuracy of the linearizer, can be estimated as $\pm$ 3%.

7) Temperature Variations

Temperature did not change more than $\pm 3^{o}$ during a test run.

8) Boundary Layer Data Accuracy

The accuracy of the traversing equipment was not as precise as detailed boundary layer measurements require; in particular, it was

difficult to locate the exact distance from the wall. Finally, the number of data points taken in the boundary layers were not sufficient for a complete boundary layer analysis. For these reasons, only a few figures give boundary layer data. Generally speaking, only the wake and the free stream flows will be discussed.

3. EXPERIMENTAL RESULTS

3.1. Nomenclature

We shall call, in the following discussion, with reference to both diffusers:

Station	Distance From Inlet [i.e. From Sphere Center]	Min. Distance From Sphere Surface
X-1	0.2"	0.045"
X-2	0.5"	0.345"
X-3	1"	0.845"
X-4	3"	2.845"
X-5	5"	4.845"

Similarly we shall define:

Symbol	Oscillation Period	Oscillation Frequency
T-1	110 msec	9.09 cycles/sec
T-2	36 msec	27.77 cycles/sec
T-3	16.6 msec	60.24 cycles/sec
T-4	12 msec	83.33 cycles/sec
T-5	7 msec	142.86 cycles/sec

3.2. Mean Flow Parameters

The time mean velocity horizontal traverses are presented in figure 6 for both diffusers. As already pointed out (see Table 1) the Reynolds number for the 6^{o} diffuser was slightly higher than the one for the 10^{o} diffuser. However, in this range of Reynolds number, the flow behavior should be relatively insensitive to variations of Reynolds number. It can be seen that the effect of the pressure gradient is felt in a higher velocity defect for the 10^{o} diffuser which persists, for all the stations, more than in the 6^{o} diffuser.

The data points of figure 6 were exactly coincident for both oscillating and non-oscillating flows, at the same time-mean Reynolds number. No influence of the superposed frequency on the wake shape was detected. The time mean velocities shown are the reference ones for all our subsequent measurements of the turbulence intensities and oscillation amplitudes.

The time mean static pressure behaviors in the two diffusers are presented in figure 7 as pressure difference between the local condition and the atmosphere, nondimensionalized with respect to the inlet dynamic pressure. It can be seen that, up to $x/L = 0.25$, the pressure gradients do not differ strongly between the two diffusers.

3.3. Integral Turbulence Intensities

In figures 8 through 11 the root-mean-squares of the integral turbulence (i.e. with the contributions of the superposed oscillations)

are given, with reference to the inlet time mean velocity, for the 10^{o} diffuser. The non-oscillating conditions (dashed lines) are compared with the oscillating conditions taken at T-1, T-2, and T-3. When only the dashed line appears at some locations, it means that all the oscillating conditions coincided with the steady (non-oscillating) condition. It is apparent, by examining these rms readings for oscillating turbulent wakes that the random turbulence contribution is so high, even in steady conditions, that the superposed oscillations are almost completely shadowed, in particular at locations X-1 and X-2. Throughout the figures there is the systematic tendency toward higher rms levels for lower oscillation frequencies. As can be seen in Table 1, this results from the higher $|u_i|$ produced, at these frequencies, by the oscillating value.

We want to add that, as already indicated, the readings in the boundary layers are not very accurate. Nevertheless it is worth pointing out the peak in rms levels shown in figure 10 in the boundary layers for the frequency T-2 which is not consistent with an actual oscillation amplitude peak (see later in figure 14). This kind of behavior falls into the domain of amplification phenomena, characteristic of boundary layers (laminar and turbulent) in diffusers, which are not dealt with in the present study but which were detected and analysed in the course of our research (see Introduction).

Figures 8 through 11 are readings from horizontal traverses and show excellent symmetry. In these figures a y/R scale has been

added at the top, for comparison purposes with the oscillation amplitude behavior presented in the following figures.

3.4. Oscillation Amplitudes

Figures 12 through 15 present amplitude ratios (i.e., local oscillation amplitudes divided by the inlet oscillation amplitudes relative to the same frequency) respectively for stations X-1, X-2, X-3, X-4 in the 10^{o} diffuser. Figures 16 through 19 present exactly the same for the 6^{o} diffuser. A useful and easy comparison is thus allowed. Although a detailed analysis of the results will be given later on (see next paragraph), we want here to stress the basic similarity of the results for the two diffusers. This, in our opinion, is very interesting because it shows that the pressure gradient is not a critical parameter for the oscillation amplitudes, with regard to either their absolute values (although with clear systematic influences) or their decay rates.

Boundary layer results are given only for comparison purposes, as they show much higher amplitudes (generally speaking) than the wake. We must not forget that a rather long cylindrical section was placed ahead of the diffuser, and the wall boundary layers could develop before entering the diffuser, whereas the boundary layers on the wake generator had little previous history and they grew in a favorable pressure gradient before being shed into the diffuser (see later). More importantly, the wake-boundary layer comparison is a free shear

layer-wall layer comparison.

General preliminary conclusions which can be done are as follows:

a) The pressure gradient does not critically control the oscillation behavior and decay rates in the near-wake.

b) In the high frequency range, higher peaks of the oscillation amplitudes in the wake flow occur at lower pressure gradients; that is, the oscillations seem to decay at a higher rate with higher axial pressure gradient.

c) For very low frequencies, no amplification relative to local free stream values occurs in the wake; rather a strong damping of oscillations takes place there.

d) For the medium and high frequencies, oscillation peaks up to (and above) twice the free-stream levels are detected.

A more detailed analysis will follow.

3.5. Oscillation Phase Relations

Figures 23 through 26 present the differences in oscillation phase between the local values and the free stream values at the same axial location and at the same frequency. The accuracy of the results is limited and is not better than $\pm 10^{o}$. It is interesting to note that absolutely no phase shifts are detected for the low frequencies, that strong negative phase shifts occur at the beginning of the near-wake with preference for the high frequencies and that there is a tendency

toward positive shifts as the wake develops, with a clear preference for an intermediate frequency, the same frequency which appears as the dominant one for the oscillation amplitudes in the region farther away from the wake generator. The results for both diffuser are absolutely consistent. No data for the boundary layers is presented. For the outer parts of the boundary layers negative shifts were always detected.

4. MECHANICS OF THE OSCILLATION GENERATION AND DECAY

To reach a clearer description of the phenomena which are supposed to occur starting from the point at which the flow encounters the wake generator (sphere), let us divide the flow field into four regions:

1) Oscillating boundary layer on the sphere surface.

2) Laminar (or turbulent) separation region.

3) Near-wake region.

4) Far-wake region.

Our experimental data deal mainly with the near-wake and not at all with regions 1) and 2). However, the available results are sufficient, in our opinion, to give a reasonable explanation of what is going on. Let us begin with an analysis of figures 20 and 22 which present results taken from figures 12 through 19 respectively at the centerline (y/R = 0) and at the peaks of the oscillation amplitudes for each axial station and for both diffusers. The sharp contrast of the

amplitude ratio behavior between the two figures is apparent. Figure 20 presents, in the high frequency range, clear secondary peaks, after an initial decay, for the amplitude ratio; whereas figure 22 shows a continuously decaying behavior. From figure 20, we should conclude that wakes, in their core flow, do indeed amplify (in the axial direction), all the oscillations, except the low frequency ones. This amplification takes place after an initial decay and reaches a peak which is higher and closer to the wake generator for increasing values of frequency. All this is quite clear for the high frequencies, but it is also valid for the medium frequency curves too, if we pay attention to their positive slopes, instead of negative, going down stream of the initial peaks.

However, at this point, a closer look at the same figure 20 and a comparison with figures 21 and 22 show that a different trend occurs for the plot of the maximum amplification ratio versus axial distance. First of all, comparing figures 20 and 21, we can see that the initial peaks for the T-2, T-3 frequency curves are not higher than the free stream amplitudes for those frequencies. That is, no amplification with respect to the free stream takes place there. True peaks, with respect to the free stream, are instead those for the T-4 and T-5 frequency curves, together with the positive slopes of the T-3 curves. But now, analyzing figure 22 we realize that all the aforementioned peaks fall, at each station, below the maximum of the oscillation

amplitude. These maxima always decay with axial distance and are located in the "oscillation layers" which separate the wake core (shielded region) directly behind the sphere and the free stream region. It is in these layers that rather high amplitude ratios are detected, although they steadily decrease going away from the wake generator. These amplifications are the highest for the frequency T-4 and show consistent behavior for the two diffusers, with systematic higher values for the lower pressure gradient.

The curve for frequency T-5 is not continuous because near the peaks at station X-2 the results for both diffusers showed random signals and no amplitude could be calculated. We feel that this phenomenon was caused by inertia effects: as it is also pointed out in reference [5] , wall boundary layers and free shear layers cannot follow the oscillations in the free stream, when the frequency of the oscillations is above a certain limit, because of the inertia of the fluid particles together with the influence of the turbulence level.

It is clear that, in the time mean shear region of the near-wake, superposed oscillations of any frequency are damped out in the axial direction at a rate which is higher the closer to the wake generator. The rate of damping is also dependent on frequency: it reaches a maximum for a frequency around T-4.

A better understanding of oscillation behavior in the wake shear region can be hypothesized as follows. We expect that oscillations did

amplify in region 1), the boundary layer on the sphere upstream surface, for the following reasons:

a) Peaks in velocity amplitudes can be expected to occur in both laminar and turbulent boundary layers subjected to oscillatory free stream flows, due to the fact that, after a change in the free stream velocity, the velocity in the boundary layer, at each location, has two components of change, one coming from the variation in free stream velocity, the other generated by the change of thickness of the boundary layer itself (see [2]).

b) The wall skin friction coefficient is fluctuating in response to the organized disturbances in the free stream. From [5] we see results which confirm the variation of the root-mean-square fluctuating skin friction with disturbance frequency. In particular, at relatively large disturbance wavelengths an increase in disturbance frequency is accompanied by an increase in the rms fluctuating skin friction. However, as the frequency increases further, changes in the disturbance pressure gradient become more rapid, until a point is reached at which inertial effects come into play, this fact being the expected reason of the lack of response of the boundary layer to further decreases in disturbance wavelengths (see [5]).

This phenomenon can also shed light on the trends shown in figure 22. The oscillation amplitude is maximum at T-4 whereas it decreases at frequency T-5. As far as the phase is concerned, typical

results from [5] show that in the low frequency range the fluctuating skin friction is in phase with the free stream disturbances since the boundary layer can adjust to the instantaneous conditions. However, if the disturbance is of high frequency, the above adjustment cannot take place and phase discrepancies as well as distortions in wave form will begin to appear. In these conditions, the fluctuating skin friction appears to anticipate the inviscid flow disturbances in the inner portion of the boundary layer due to its relatively low inertia, which results in a greater relative change of velocity in the boundary layer than in the free stream.

We have not measured the characteristics of the boundary layer which developed on the upstream portion of the sphere, but we can rather safely assume it to be laminar, regardless of the superposed oscillation frequency, due to both the low Reynolds number evaluated for the sphere (see Table 1)and the favorable pressure gradient acting on it, together with a particularly smooth sphere surface (polished steel). Therefore we expect a laminar separation to have occurred somewhere, possibly not far from the point of minimum pressure, right at the maximum cross section of the sphere located at the inlet of the diffuser. This separation onset region may certainly have been affected by the superposed oscillation amplitude and frequency, but, in any case, we can expect there little or no damping of the fluctuations developed in the boundary layer. This is due to the pulsations

of the skin friction at the surface, directly related, at the point of separation ($\tau_w = 0$), to fluctuations in the process of "shedding" the oscillating sphere boundary layer. In other words, the process of fluctuating separation can be depicted as being "tuned" (i.e. both processes governed by the same cause) with the oscillations developed upstream. If this is the case, the above explains the origin of the high amplitudes that were detected experimentally in the oscillating layers right behind the sphere, amplitudes which were then the result of two successive processes. The first process occurring in the sphere boundary layer, the second in the separation "shedding" region.

At this point, our experimental data begin to reflect behavior of the flow past the sphere. Figures 12 and 16 show, for station X-1, that in the shielded region near the centerline, for the lower frequencies, the oscillation amplitudes are lower not only than those in the oscillation layers but even than those in the free stream. This trend is pronounced and independent of the axial pressure gradient. For medium frequencies (T-3) the centerline amplitudes are comparable with the free stream ones; for the high frequencies (T-4, T-5) they are higher. The shielding effect of the sphere is apparent, and also its behavior with respect to frequency is clear: an increased frequency means higher pressure gradients in the free stream, which therefore allow the oscillations to better penetrate toward the centerline.

We have left aside the oscillation layers between the free stream and the "shielded" region. In them, except for the very low frequency, strong amplification phenomena have taken place upstream and thus their amplitudes are higher than both the free stream and the wake center amplitudes. The amplified oscillations seem to persist, in them, with a frequency response which is the highest around frequency T-4. Possibly, inertia effects together with compressibility effects prevented further amplification from occurring at higher frequencies. No critical role seems to be played by the pressure gradient, except that the amplification ratios appear some higher for lower pressure gradients. As far as the phase of the oscillations is concerned figure 23 shows strong negative phase lags in the oscillation layers for frequency T-5, less for T-4 and none for lower frequencies. The effect is less felt in the wake core.

Going downstream, we see in figures 13 and 17 an evident proof of the trends already discussed, with the particular behavior of the curves at T-5, in the oscillation layers, where the measurements of the oscillation amplitudes turned out to be prevented by a very high "dispersion" of the signals. It is worth noting that, since the oscillation decay rates are the highest at frequency T-4 and much less at lower frequencies, the peaks for frequencies T-4 and T-3 are, already at station X-2, of comparable magnitude whereas the former were much higher at X-1. The role of the pressure gradient in decreasing, with

its increase, the oscillation peaks is confirmed, but the free stream amplitudes do not seem to be affected by it. The spreading of the oscillation layers away from the centerline is apparent as was also shown in the turbulence rms traverses. Important to be stressed, in this connection, is the total absence of meaningful information we can extract from the rms readings as far as the oscillation amplitudes are concerned. Figure 9 showed a higher rms level for the wake than for the boundary layers, yet figure 13 shows instead the highest oscillations in the boundary layers. Figures 24 presents phase shifts which are negative for frequency T-4 (and less than the previous) and positive for frequency T-3.

Going now to station X-3 we find the possible explanation of the earlier mentioned secondary peaks and positive slopes detected in figure 20, whereas they did not appear in figures 21 and 22. (As previously noticed, the anomalous behavior of a curve T-2 in figure 22 depends on that kind of amplification phenomena in diffusers referred to in Introduction). The hypothesis is that the oscillation layers, coming from the sphere and carrying the highest amplitude oscillations, have spread so far that, for frequencies T-4 and T-5, they have begun to smooth out the oscillation levels in the wake core. This process has not yet occurred for the lower frequencies. The results for both diffusers are in complete agreement. In particular it is worth noting that the process of smoothing out of the oscillation layers produces, at

frequency T-4, a complete reduction of their oscillations down to the core flow value. This is not the case for frequency T-5. It is really interesting to notice that the medium frequency T-3 oscillations are decaying particularly slowly: they are, at X-3, practically constant at the levels of the previous station for the 10^{o} diffuser. The phase diagram of figure 25 shows strong positive phase shifts for frequency T-5 and negative for T-4 and T-3. No explanation could be found for this behavior. We remark that, at X-3, although the amplitude for frequency T-4 is at the free stream levels, nevertheless the phase lag is high with respect to it.

Examining now the situation at station X-4, we see that the process of smoothing of the layers has taken place for all the frequencies. Almost complete equalization of the wake oscillation amplitudes to the free stream levels has occurred for all the frequencies, except for the medium (T-3) which surprisingly persists at noticeable higher values. Apparently the dissipation energy connected with the higher frequencies has been much greater than for the lower frequene cies, together with the fact that the merging of the oscillation layers occurred later for these lower frequencies. The relatively greater persistence of the oscillations of frequency T-3 is also shown by the phase diagram figure 26 which presents positive phase shifts only for this frequency. We can indeed say that equalization conditions begin to be approached, from station X-4 on, for all but the medium T-3

frequencies. And this too seems to us rather important.

As a concluding remark we must say that, in all the above, we have neglected the influence of the difference in the inlet oscillation amplitudes with varying frequencies. This difference is not apparent in our results because they are normalized with respect to those amplitudes. Finally we specify that, from station X-1 to X-4, no detectable longitudinal phase shift was detected, i.e. the free stream oscillation phase was almost coincident, for each frequency, with the inlet free stream phase for all stations.

5. CONCLUSIONS AND SUGGESTIONS FOR FURTHER WORK

We can briefly summarize our results as follows:

1) Amplitude ratios higher than unity can be found in free shear layer flows, particularly at high frequencies. With specific reference to a near-wake, they are closely connected to oscillation amplification phenomena taking place in the boundary layer of the wake generator.

2) The rate of decay of the amplification ratios with axial distance in a near-wake is very high at high frequencies, less at lower frequencies. Intermediate frequency oscillations can thus persist amplified farther downstream.

3) Very high oscillations could be expected in the near-wakes of wake generators whose boundary layers were allowed to develop

more than in our experiments, particularly if positive pressure gradients acted on them (e.g. compressor stator blades).

4) The range of axial pressure gradients examined herein had no critical effect on the decay rates of the amplification ratios in the near-wake flow.

Checks of our results performed in larger wind tunnels at larger Reynolds numbers would be very important. A faster data acquisition and processing technique should be used. The oscillation amplitude in the free-stream should be maintained constant for all frequencies.

TABLE 1

CHARACTERISTICS PARAMETERS

	6° DIFFUSER				10° DIFFUSER			
OSCILLATION PERIODS	$\lvert u_i \rvert$ ft/sec	$\frac{\lvert u_i \rvert}{\overline{u}_i}$	St_D	St_d	$\lvert u_i \rvert$ ft/sec	$\frac{\lvert u_i \rvert}{\overline{u}_i}$	St_D	St_d
T-1 = 110 msec - - - -	0.822	0.0203	0.235	0.0364	0.795	0.0208	0.2485	0.0385
T-2 = 36 msec - - - -	0.714	0.0176	0.718	0.111	0.708	0.0185	0.76	0.1175
T-3 = 16.6 msec - - -	0.304	0.00752	1.557	0.241	0.320	0.00835	1.647	0.255
T-4 = 12 msec - - - -	0.162	0.0040	2.155	0.334	0.170	0.00444	2.28	0.3533
T-5 = 7 msec - - - -	0.112	0.00277	3.690	0.572	0.123	0.00321	3.904	0.605
REYNOLDS' NUMBERS	Re_D		Re_d		Re_D		Re_d	
All Frequencies	42,000		6500		40,000		6200	

- TABLE 2 -

LIST OF SYMBOLS FOR FIGURES 8 THROUGH 26

- ⊙ Data point at frequency T-1 in the 10° diffuser

- ◇ Data point at frequency T-2 in the 10° diffuser

- △ Data point at frequency T-3 in the 10° diffuser

- ⊡ Data point at frequency T-4 in the 10° diffuser

- ⊙ Data point at frequency T-5 in the 10° diffuser

- ⊗ Data point at frequency T-1 in the 6° diffuser

- ◈ Data point at frequency T-2 in the 6° diffuser

- ◬ Data point at frequency T-3 in the 6° diffuser

- ⊠ Data point at frequency T-4 in the 6° diffuser

- ⊗ Data point at frequency T-5 in the 6° diffuser

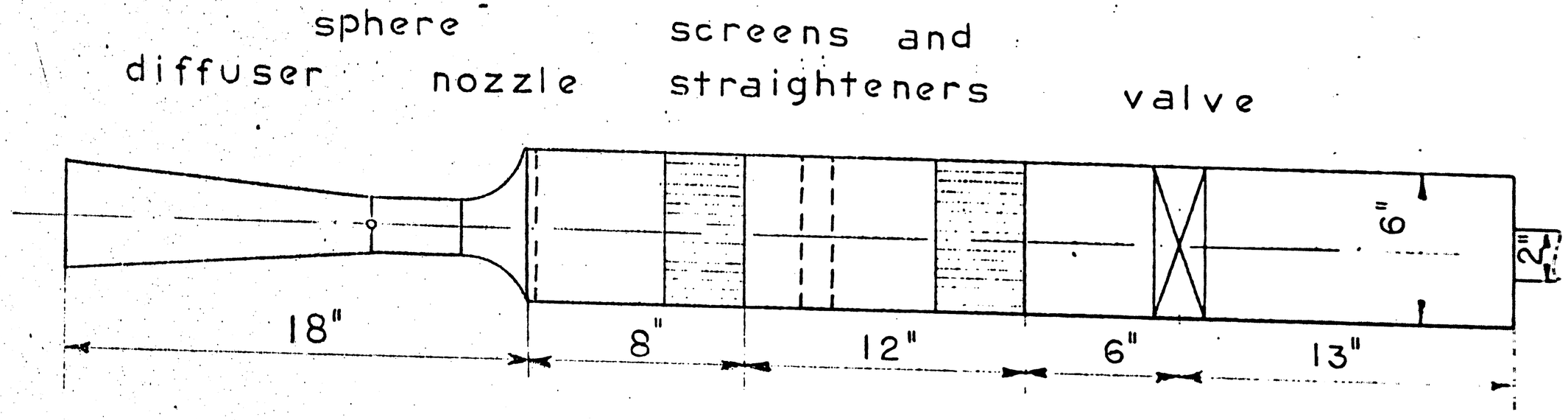

Figure 1 Wind Tunnel

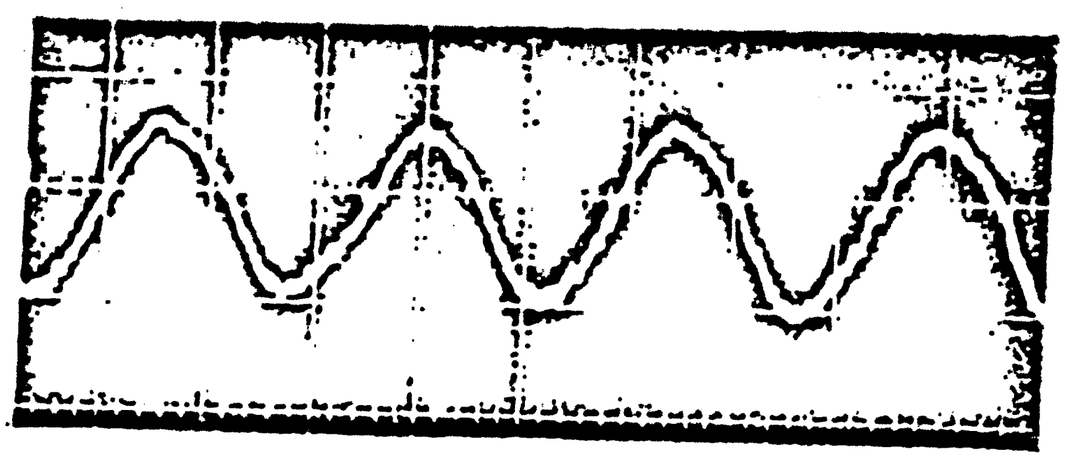

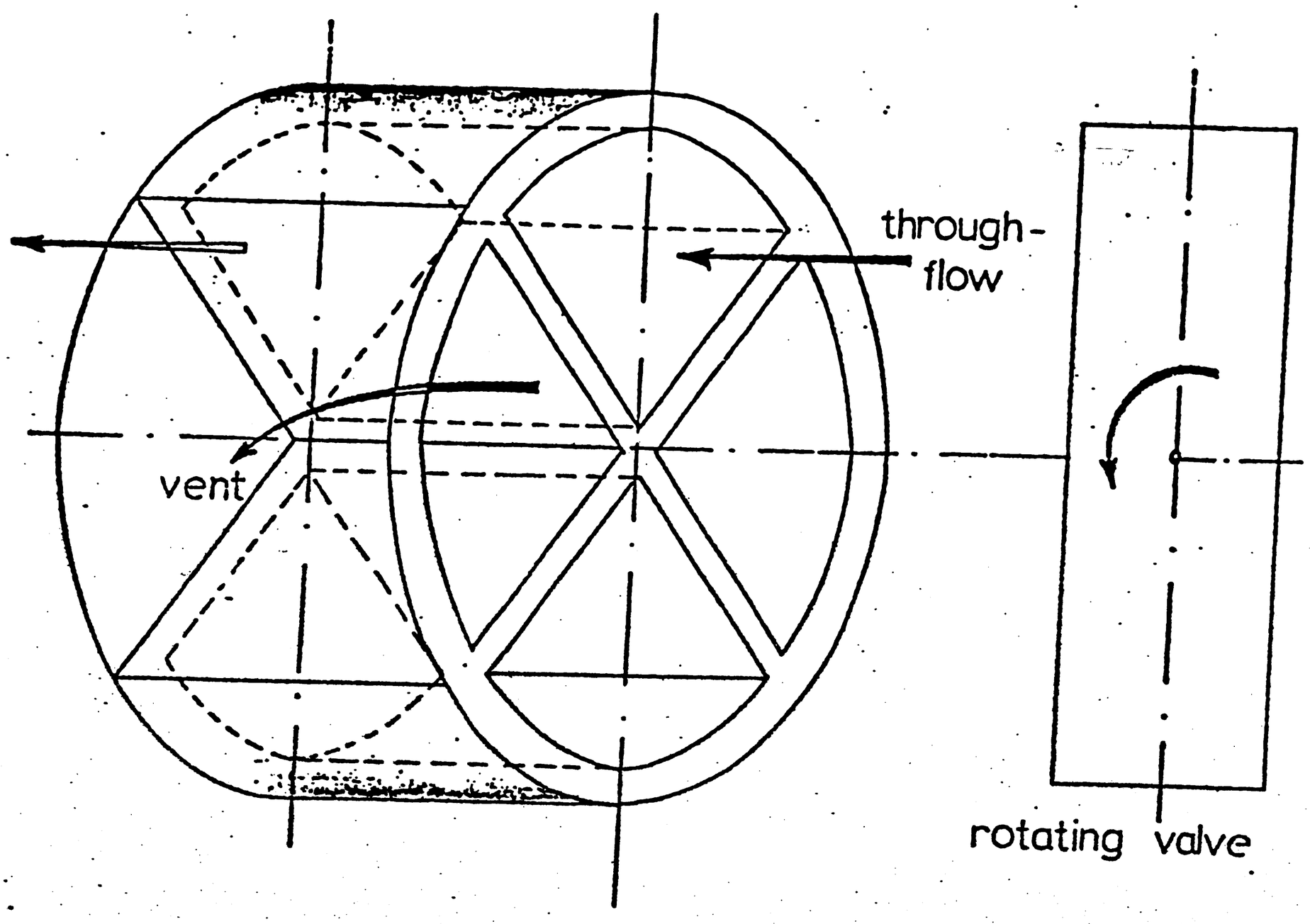

FIGURE 2 Valve Schematic

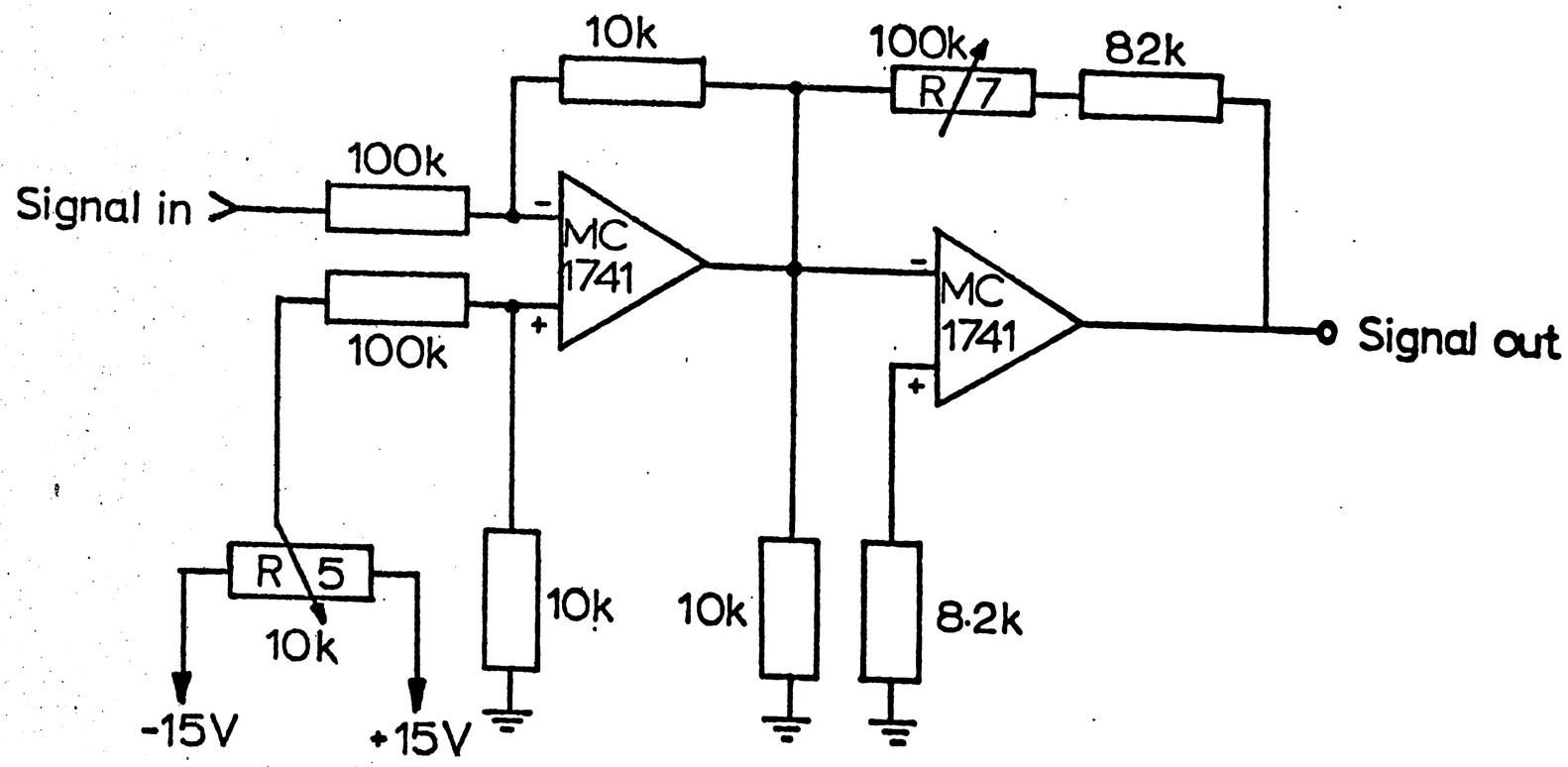

Figure 3 Zero Suppressor Circuit

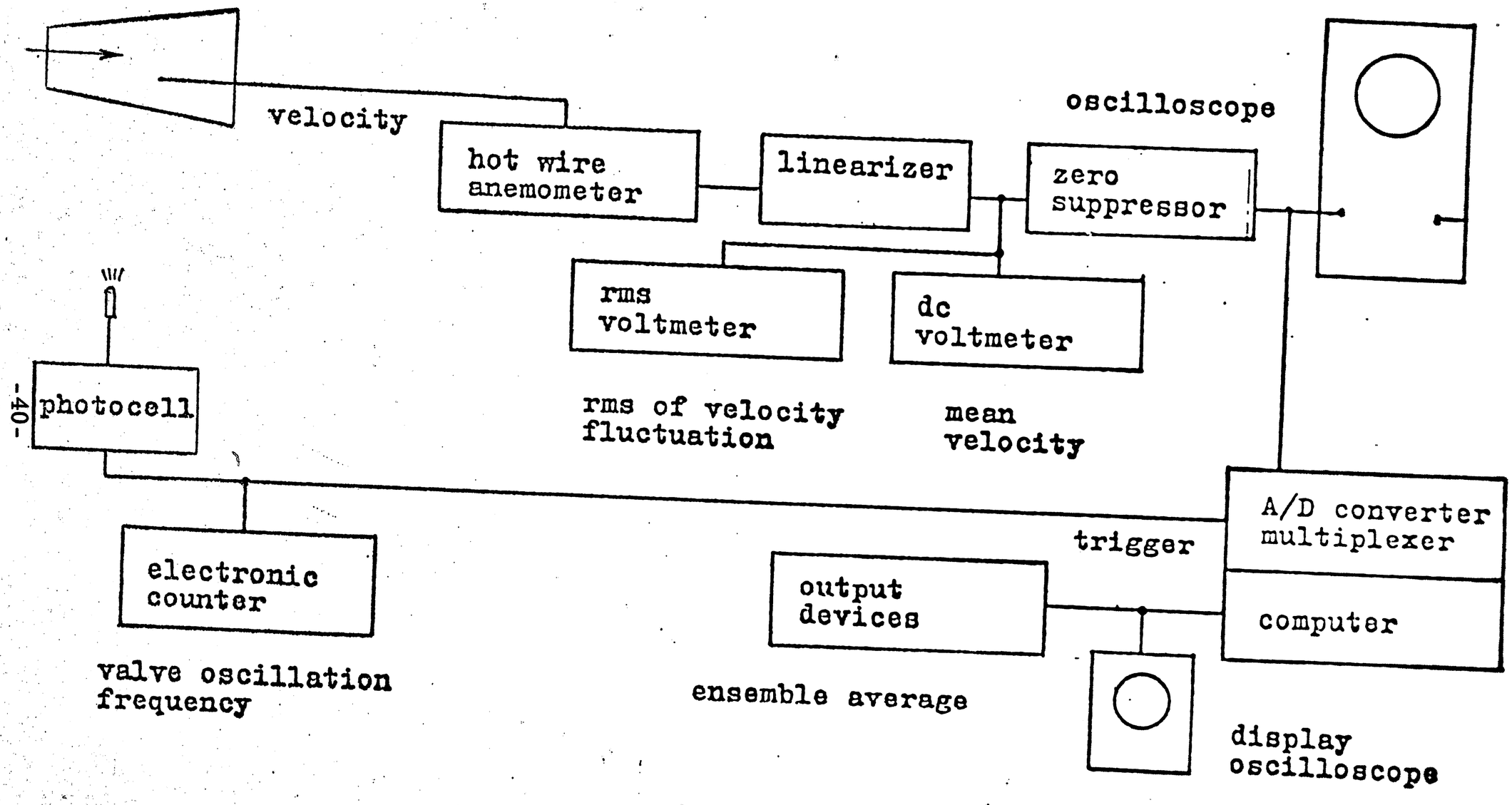

Figure 4 Instrumentation

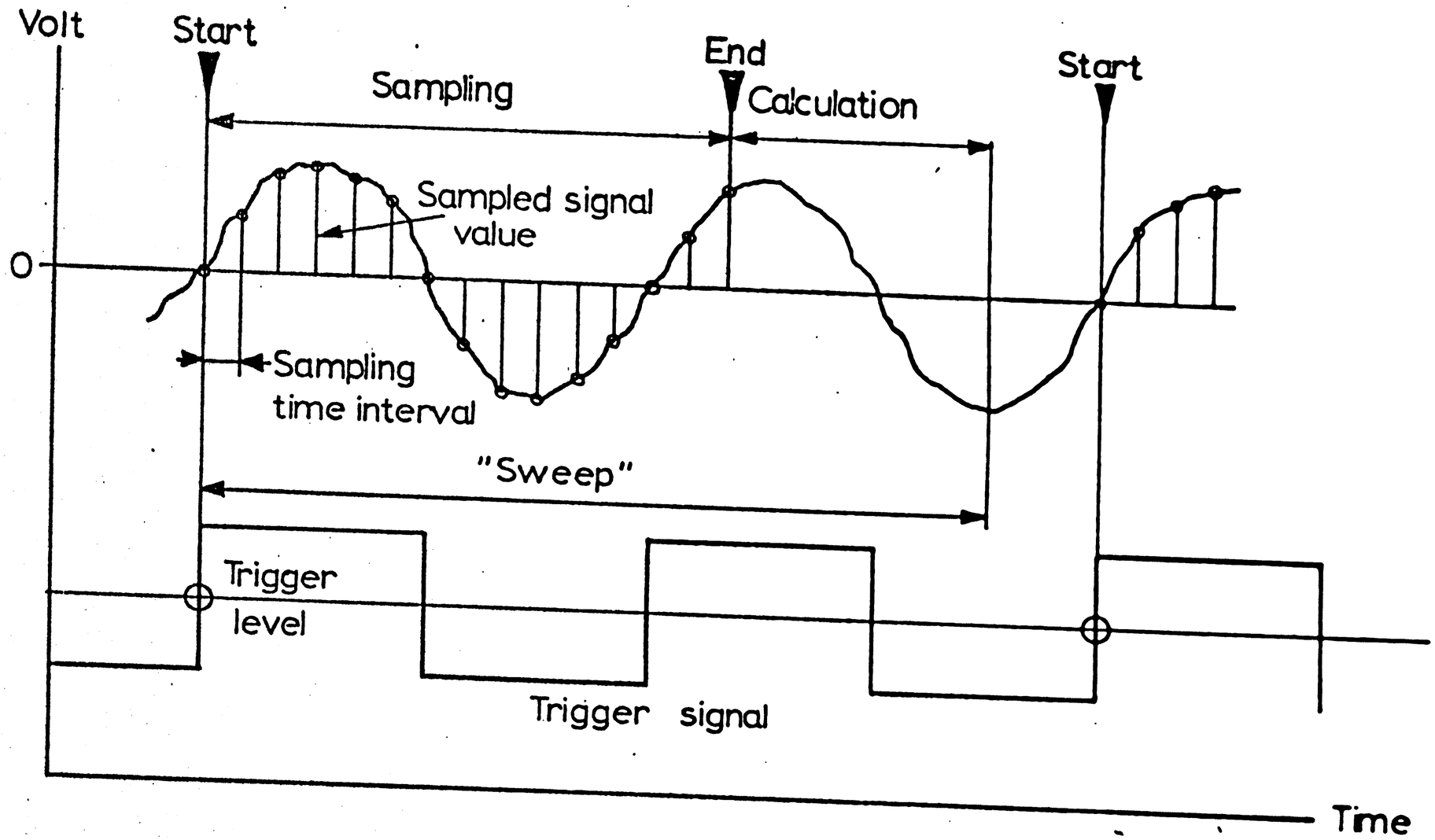

Figure 5 Averager Sampling Technique

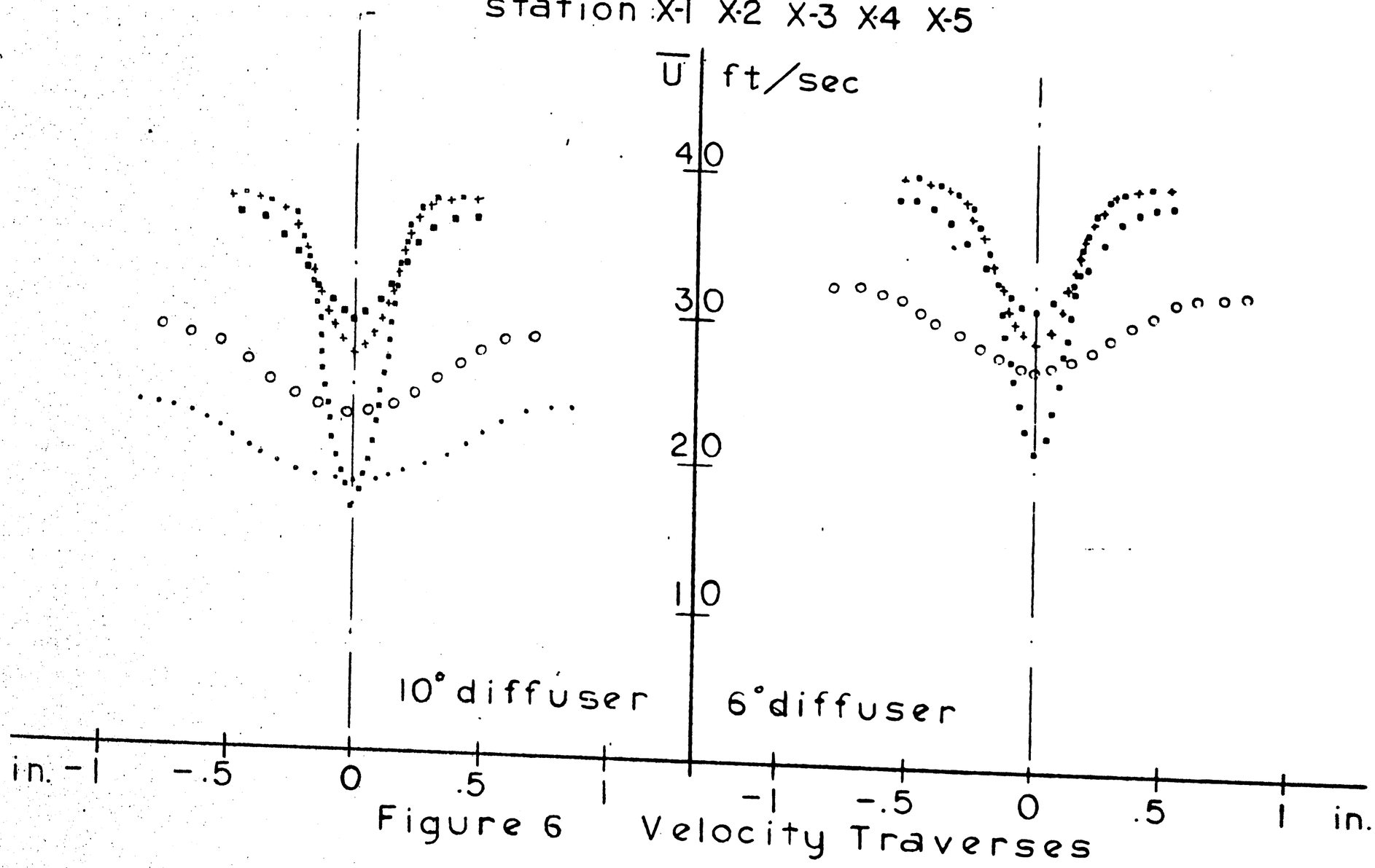

Figure 6 Velocity Traverses

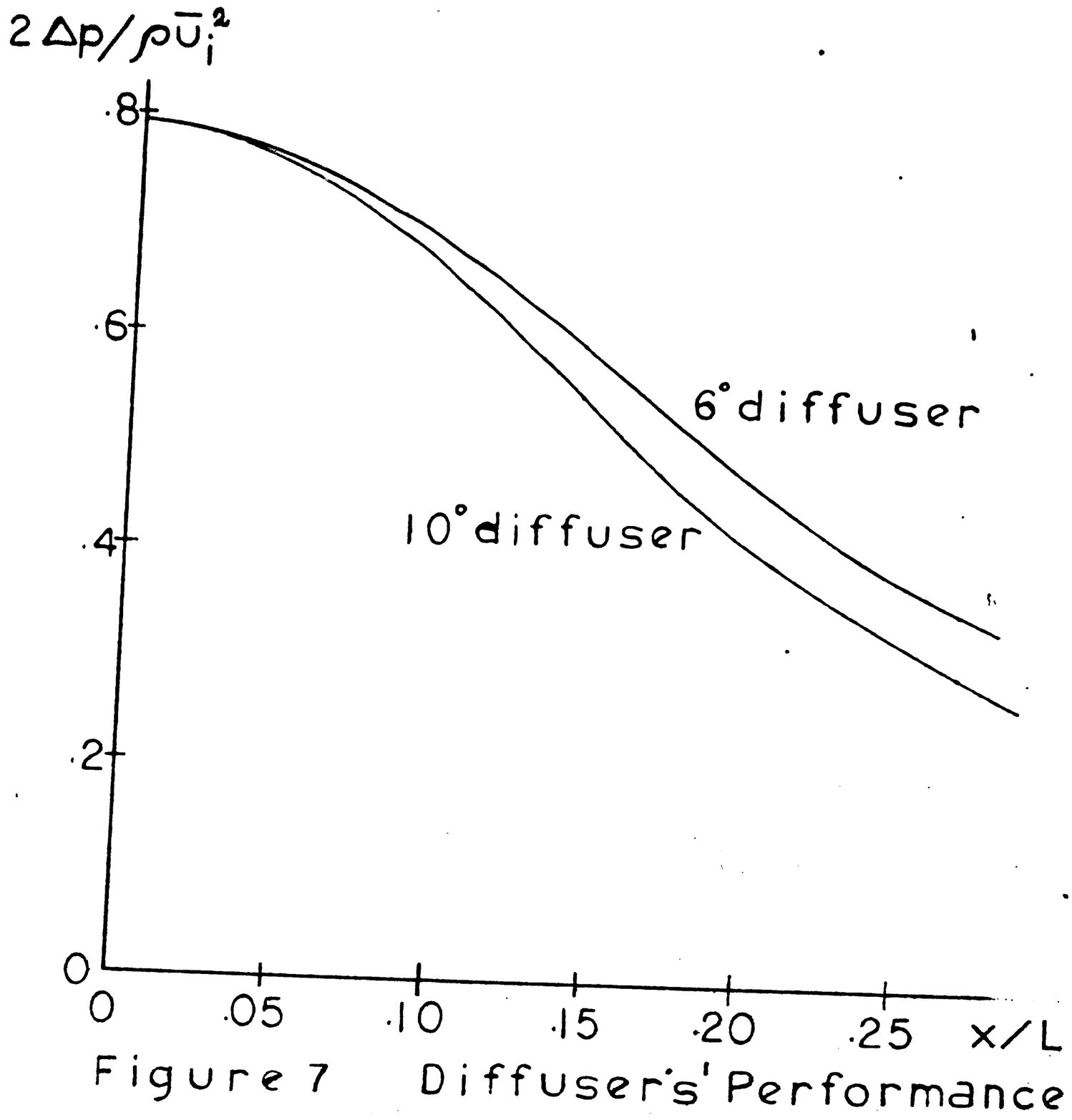

Figure 7 Diffuser's' Performance

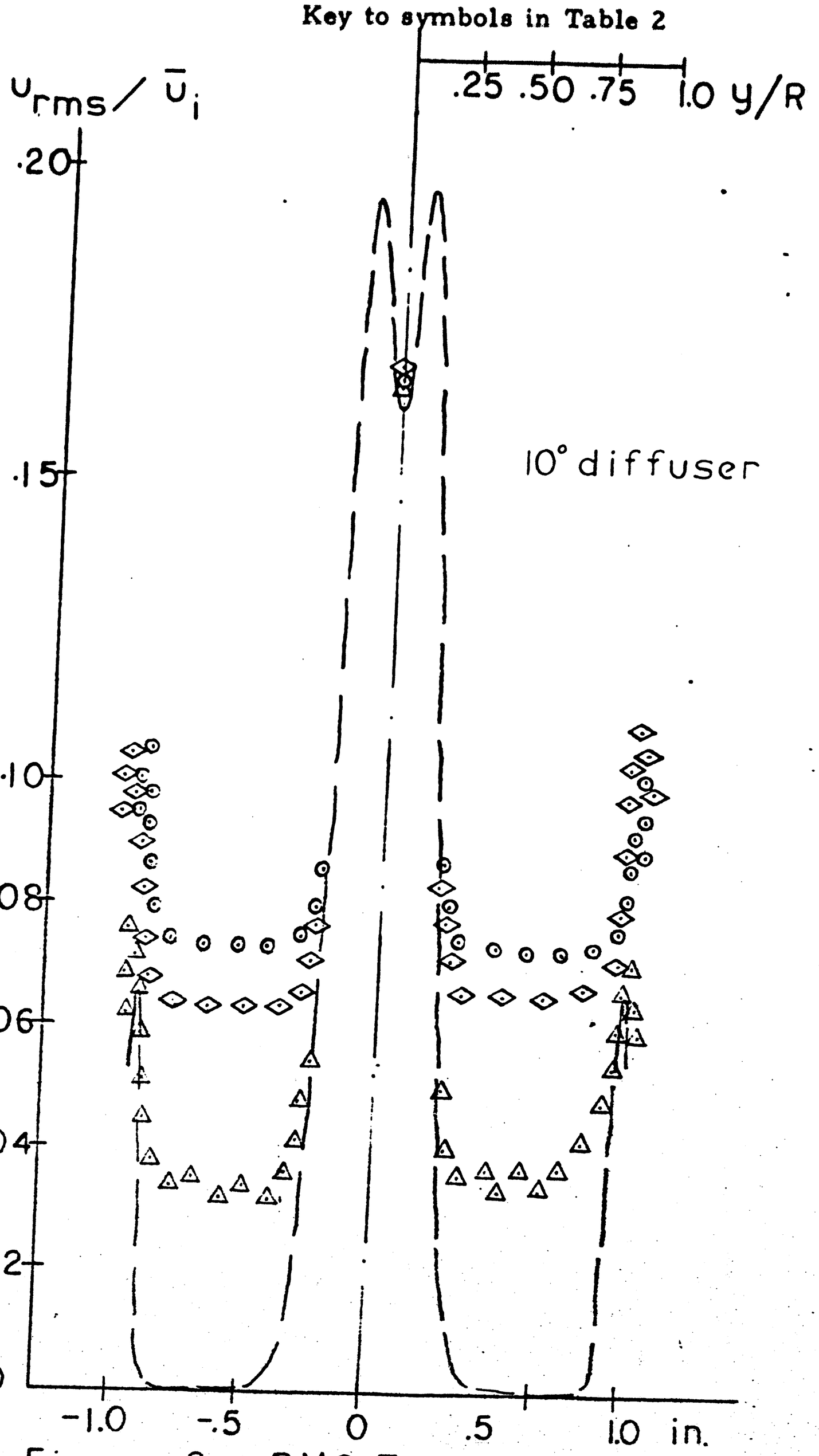

Figure 8 RMS Traverses at X-1

Key to symbols in Table 2

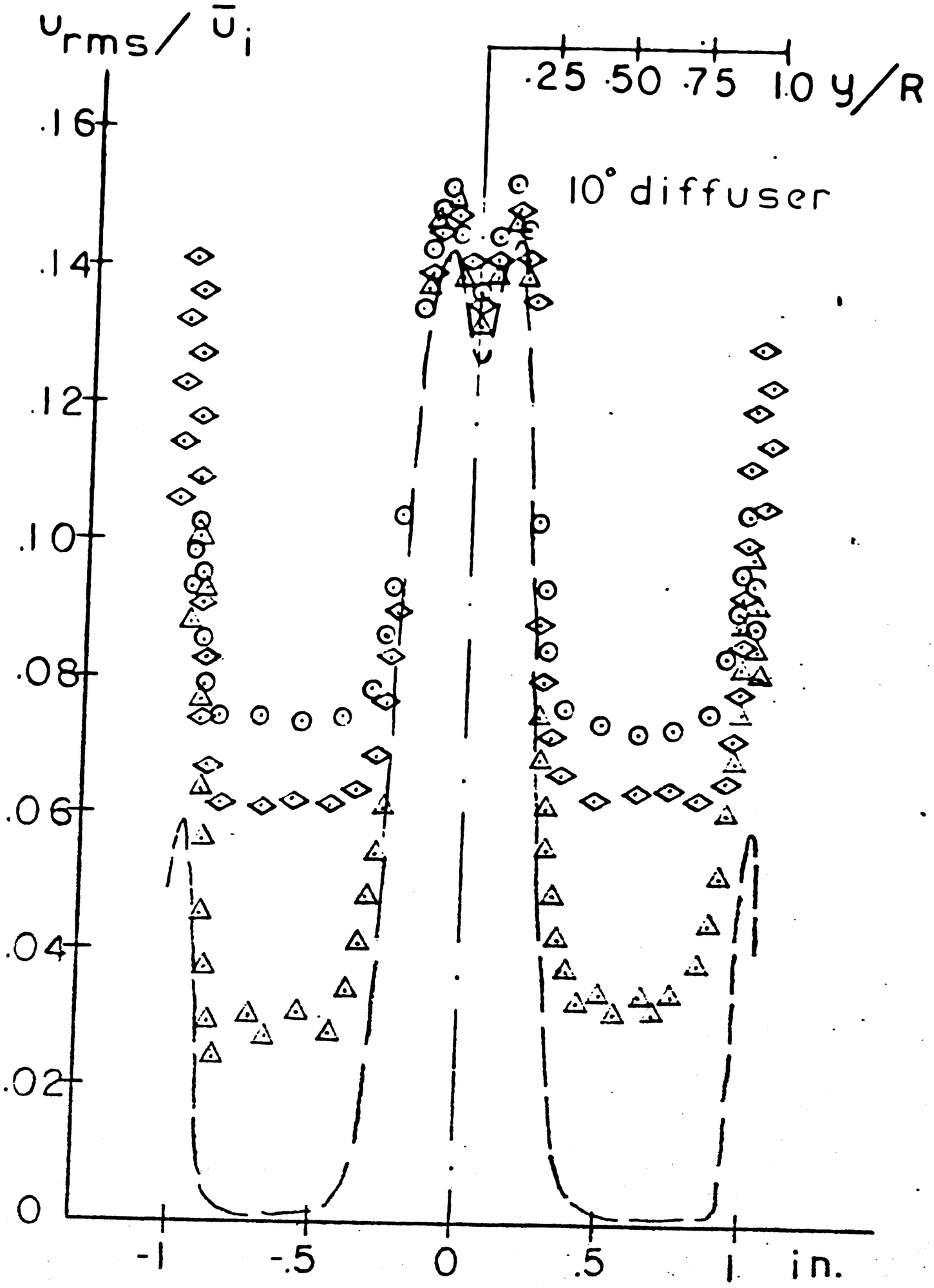

Figure 9 RMS Traverses at X-2

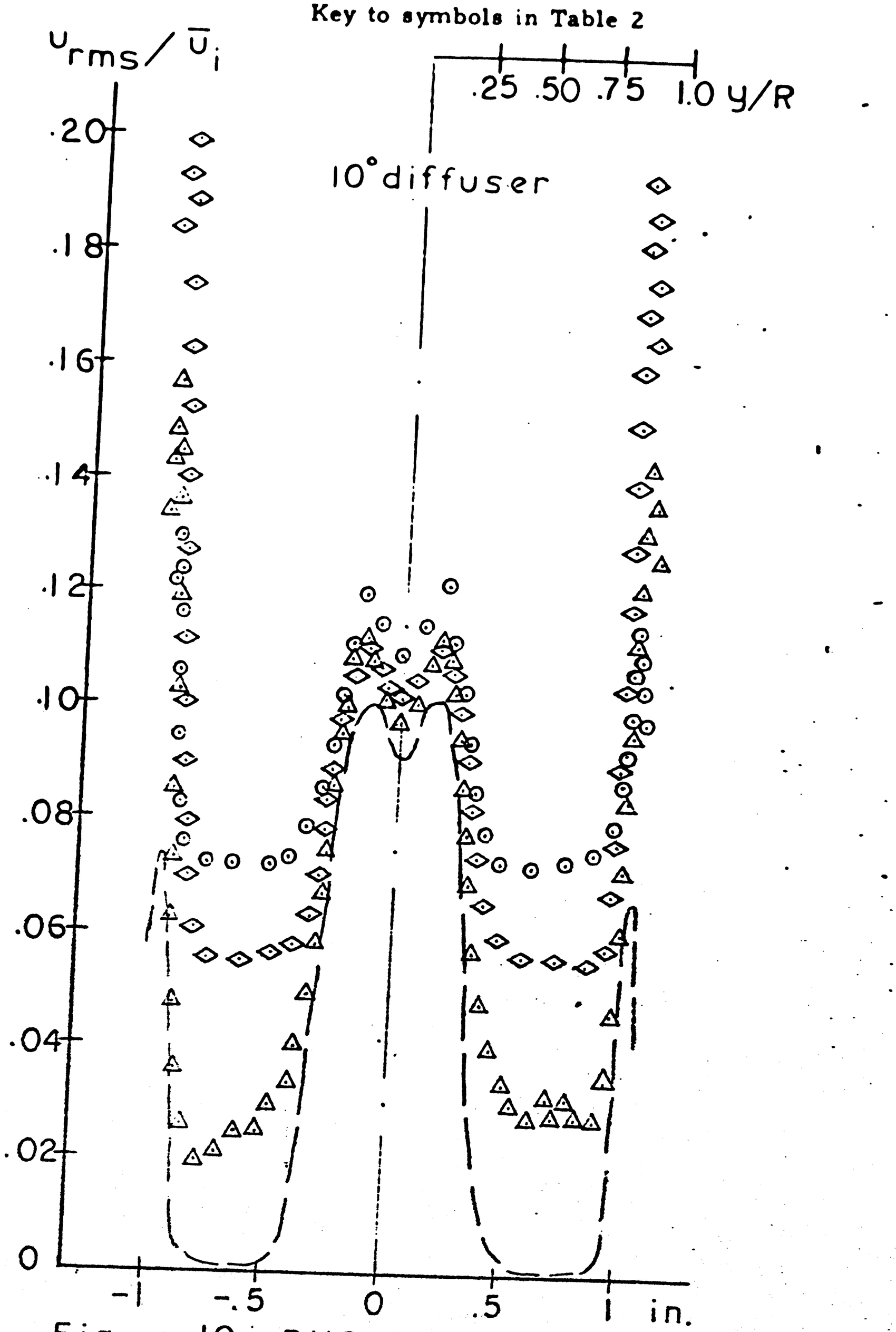

Figure 10 RMS Traverses at X-3

Key to symbols in Table 2

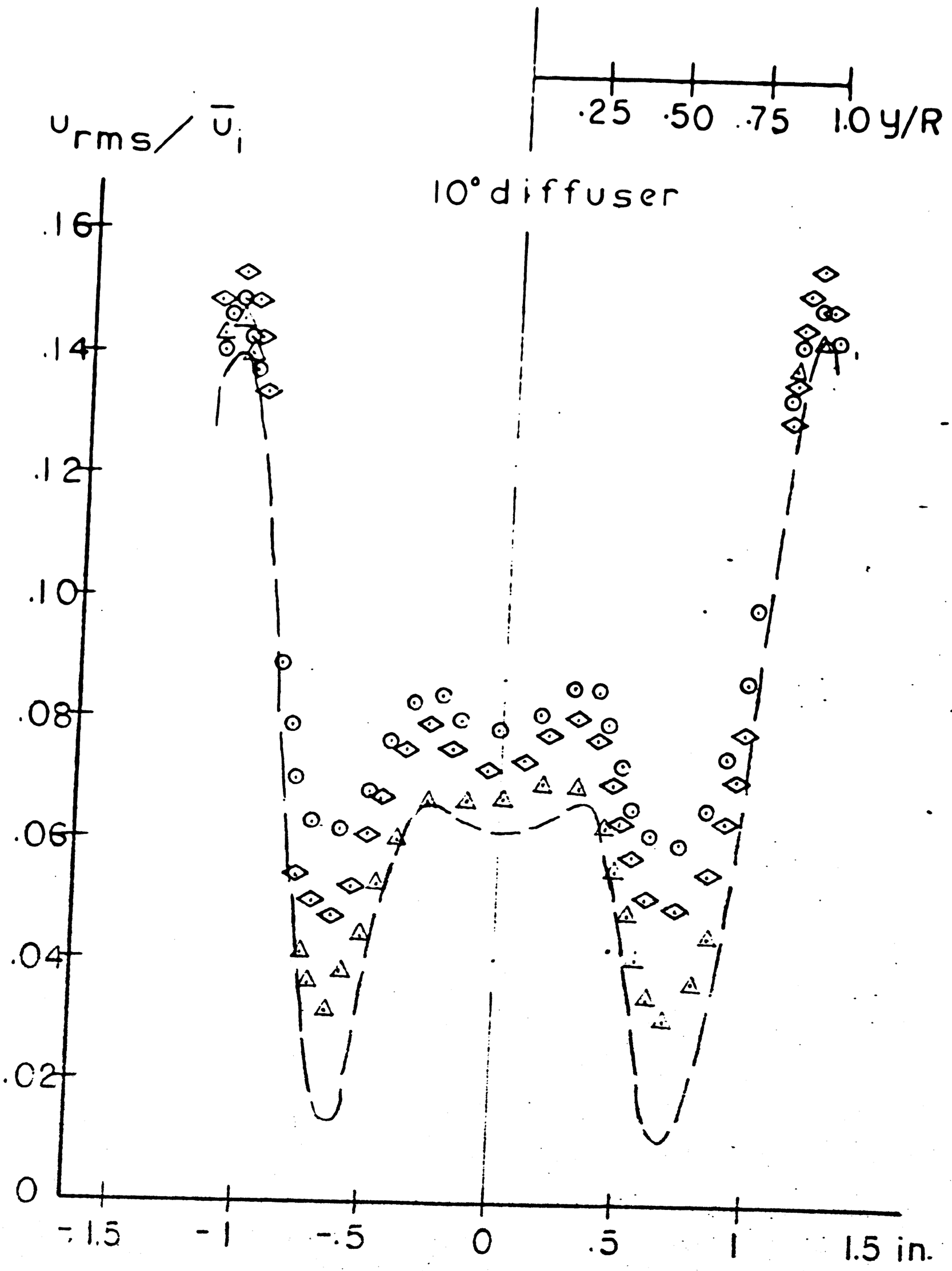

Figure 11 RMS Traverses at X-4

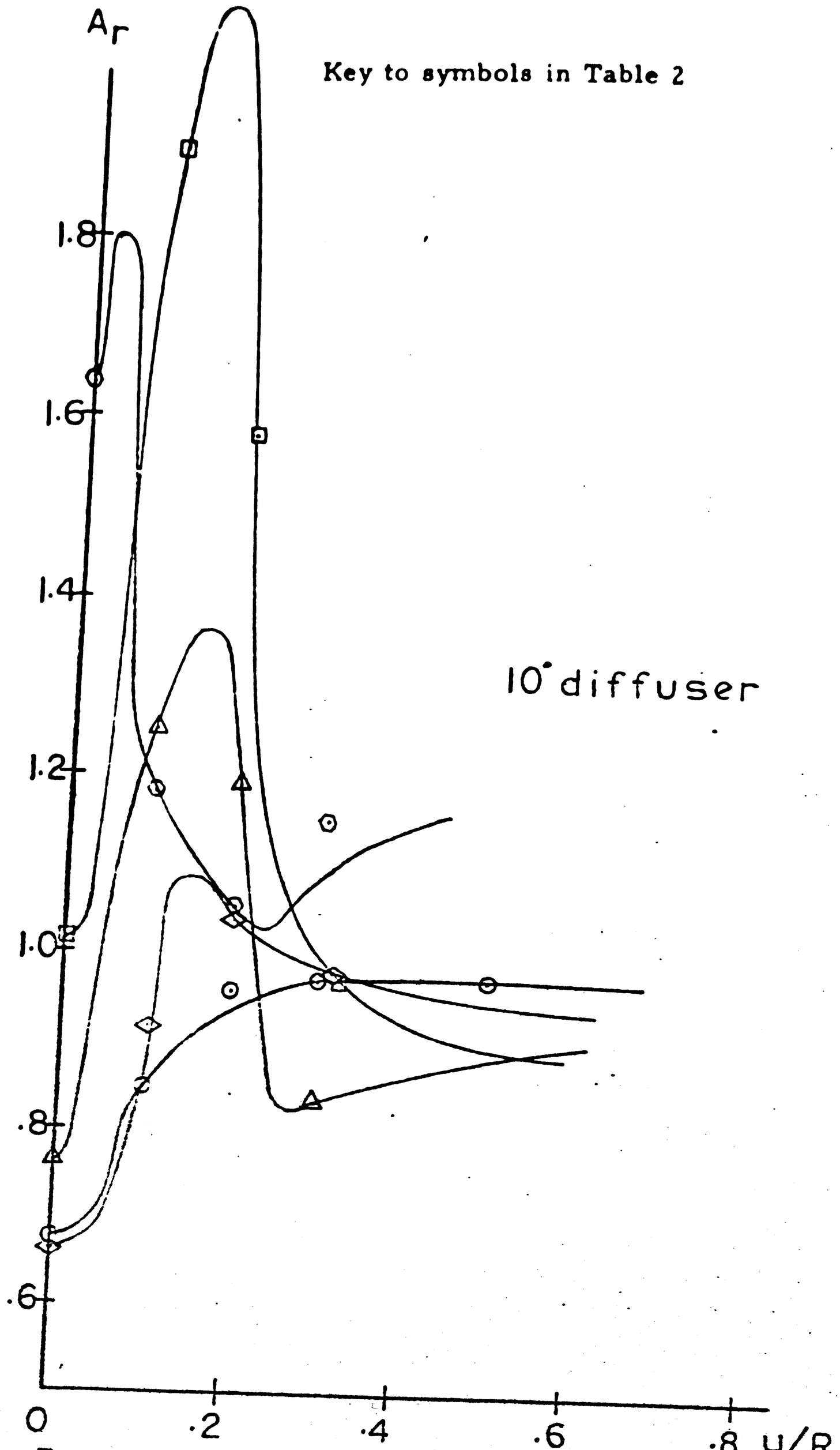

Figure 12 Amplitude Ratios at X-1

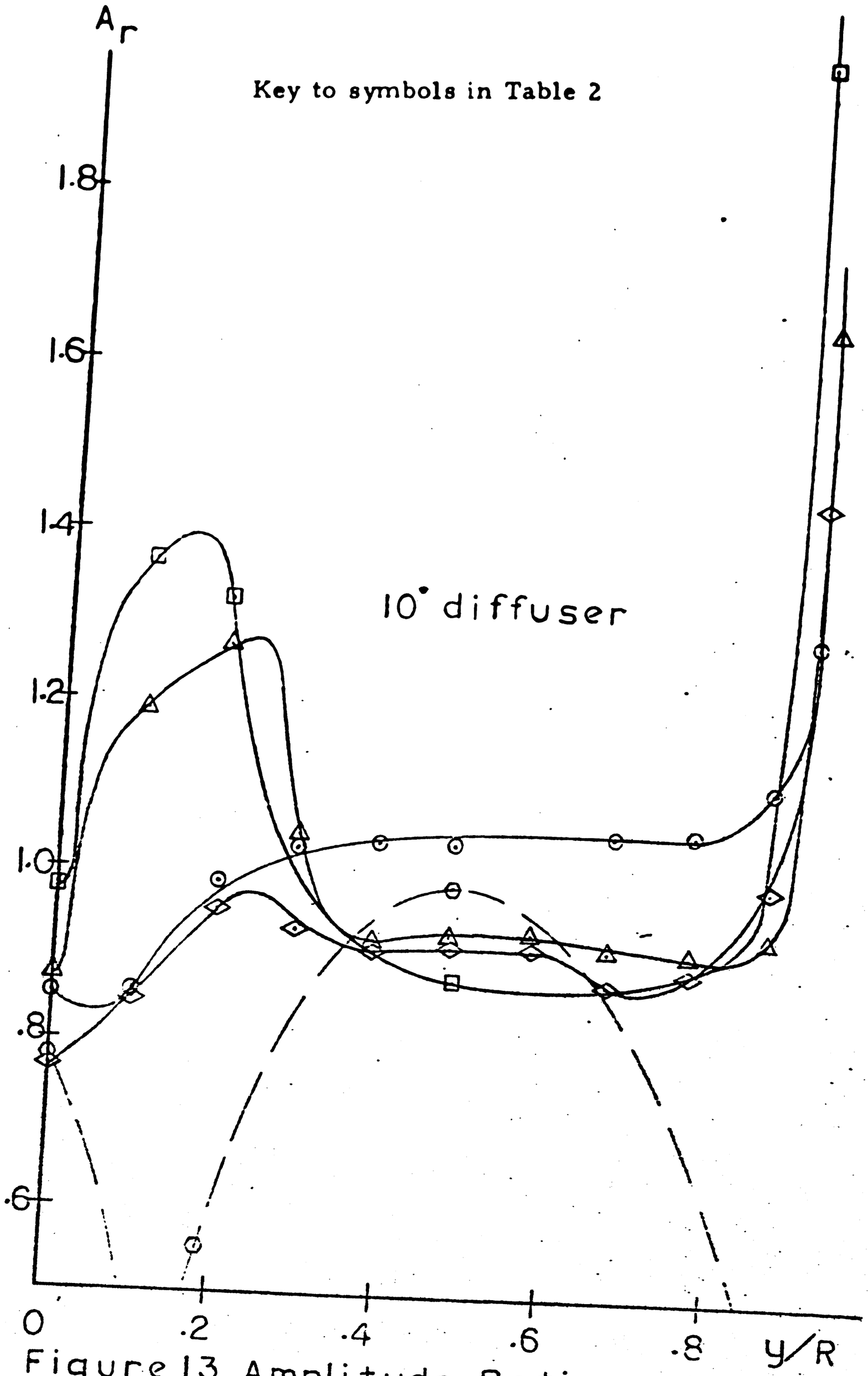

Figure 13 Amplitude Ratios at X-2

Key to symbols in Table 2

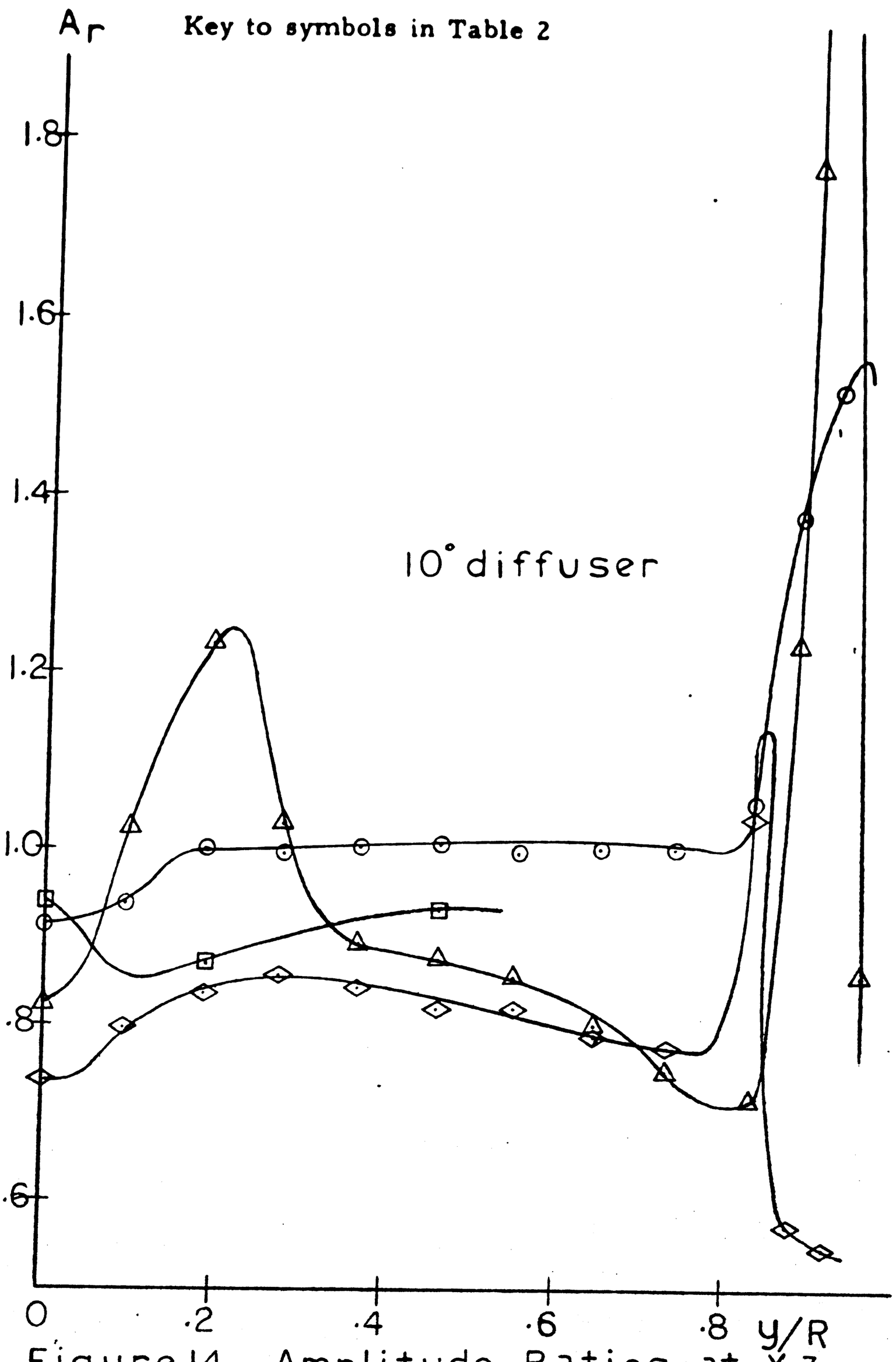

Figure 14 Amplitude Ratios at X-3

Key to symbols in Table 2

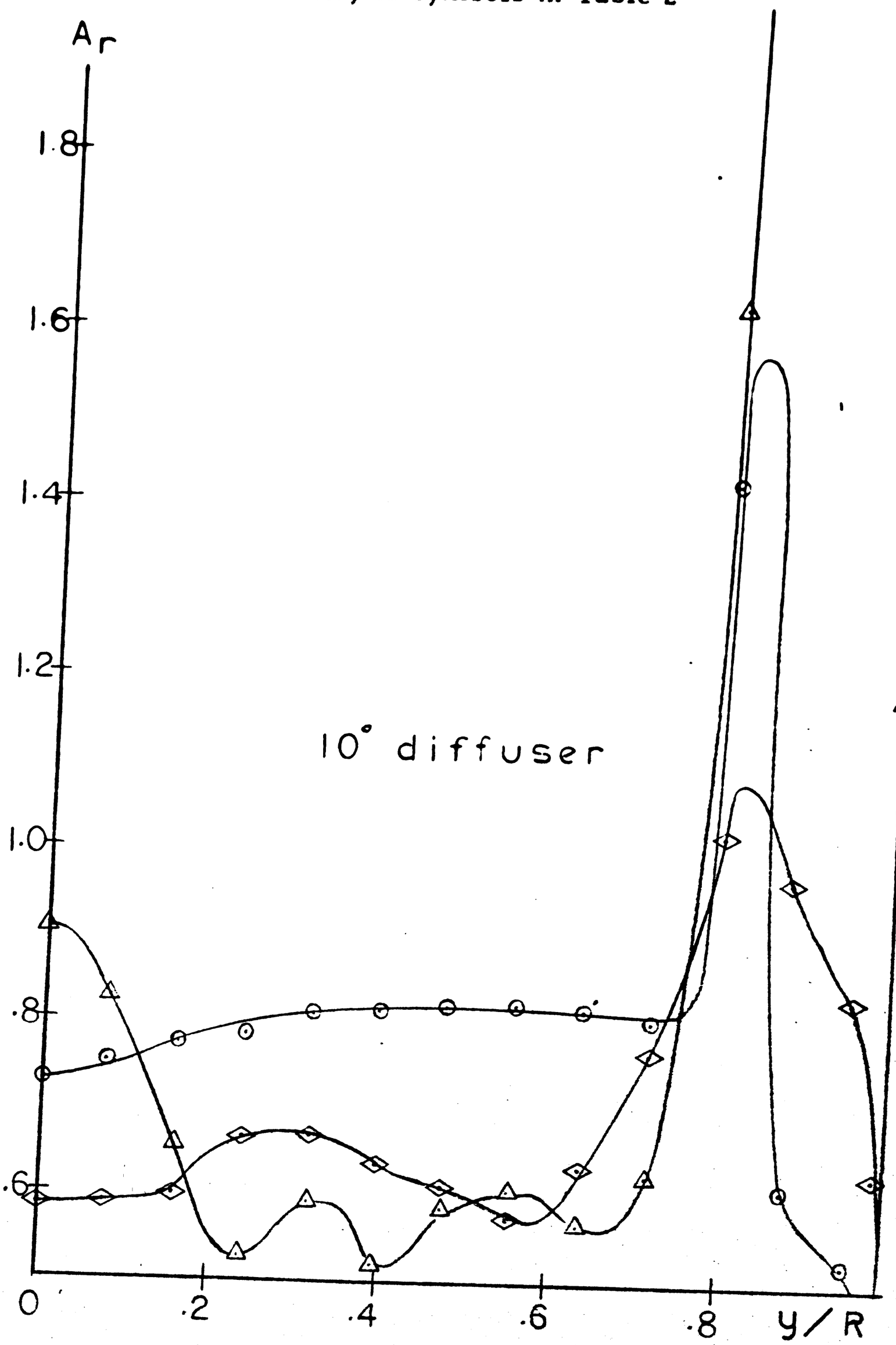

Figure 15 Amplitude Ratios at X-4

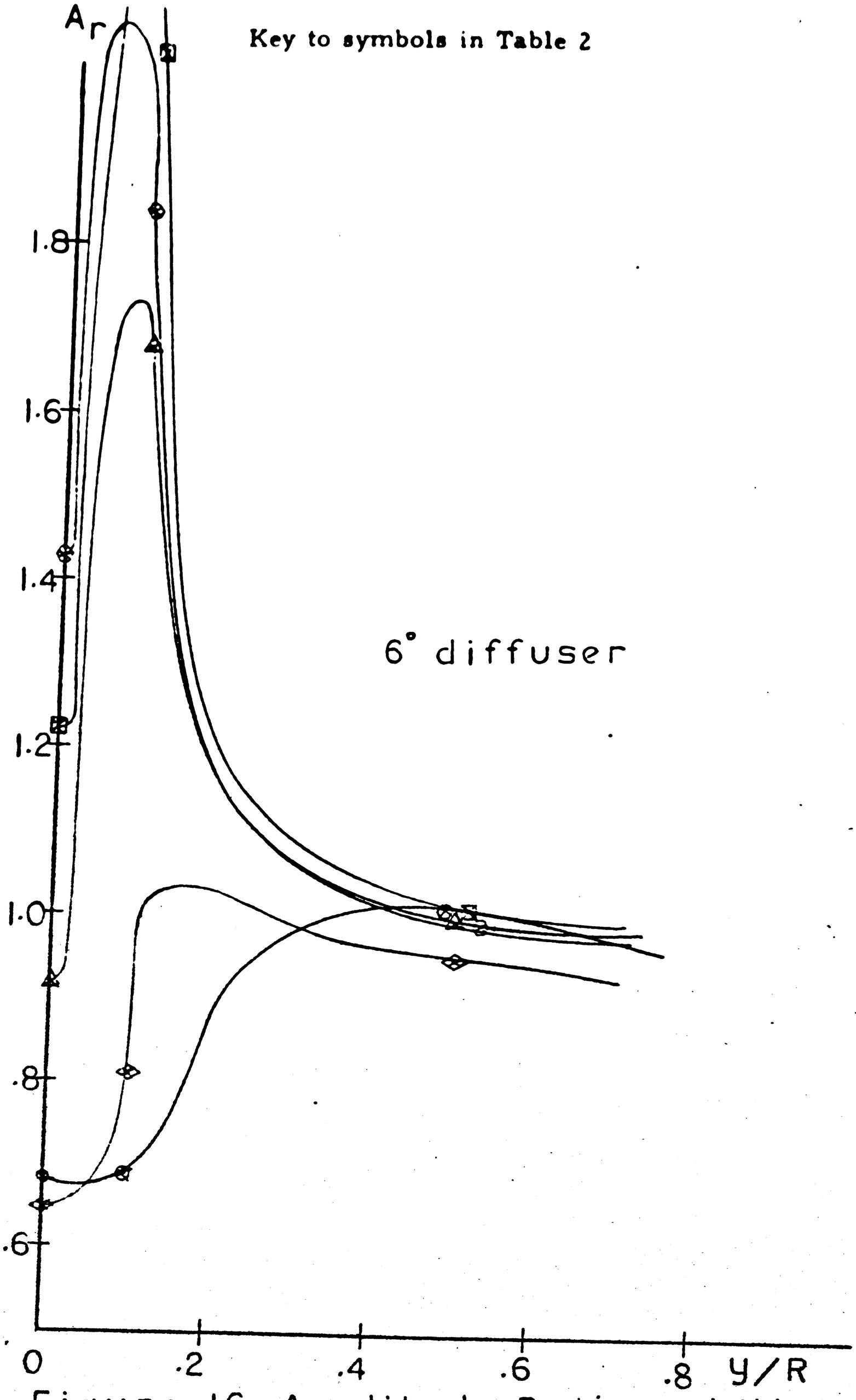

Key to symbols in Table 2

6° diffuser

Figure 16 Amplitude Ratios at X-1

Key to symbols in Table 2

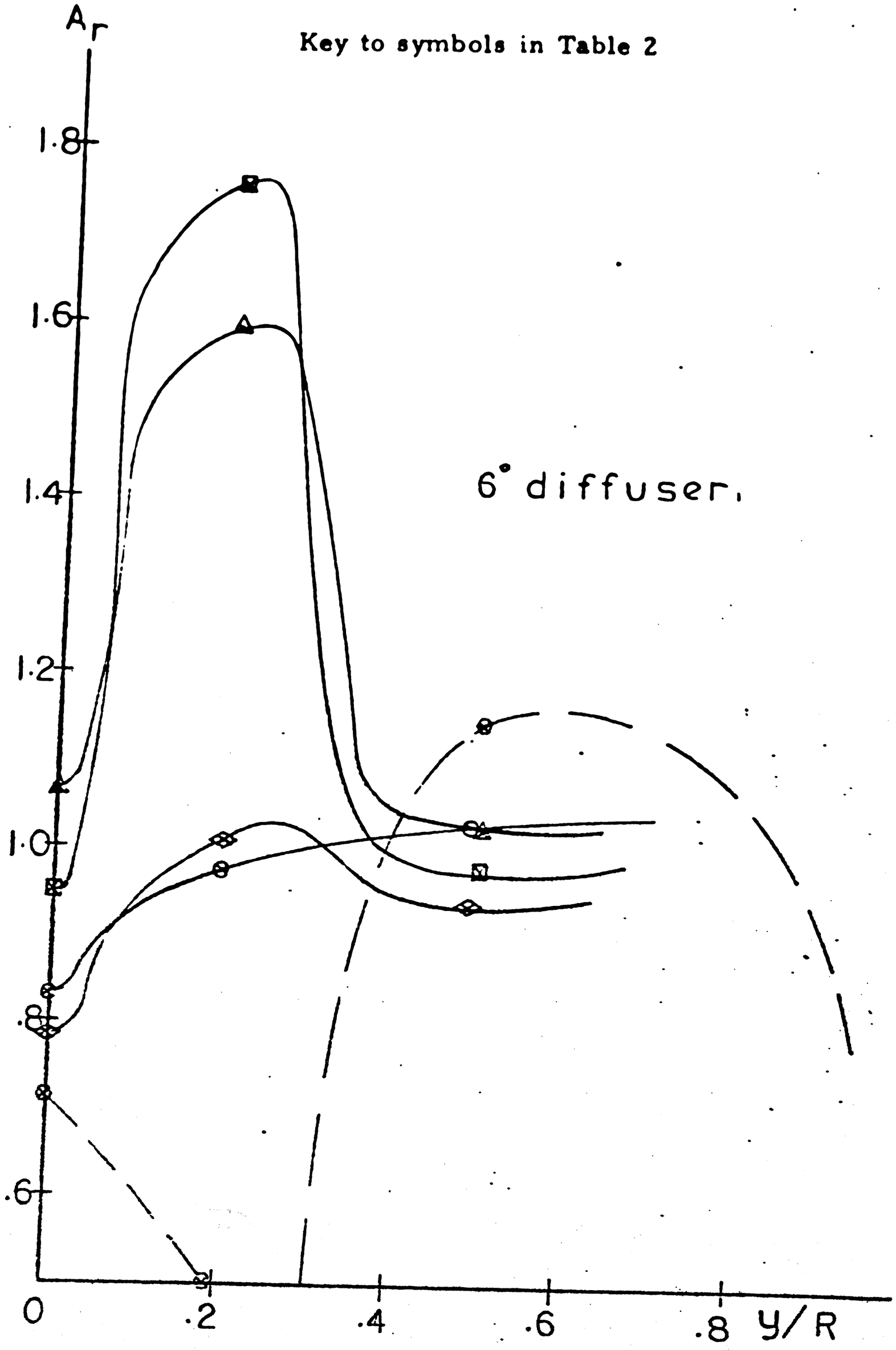

Figure 17 Amplitude Ratios at X-2

Key to symbols in Table 2

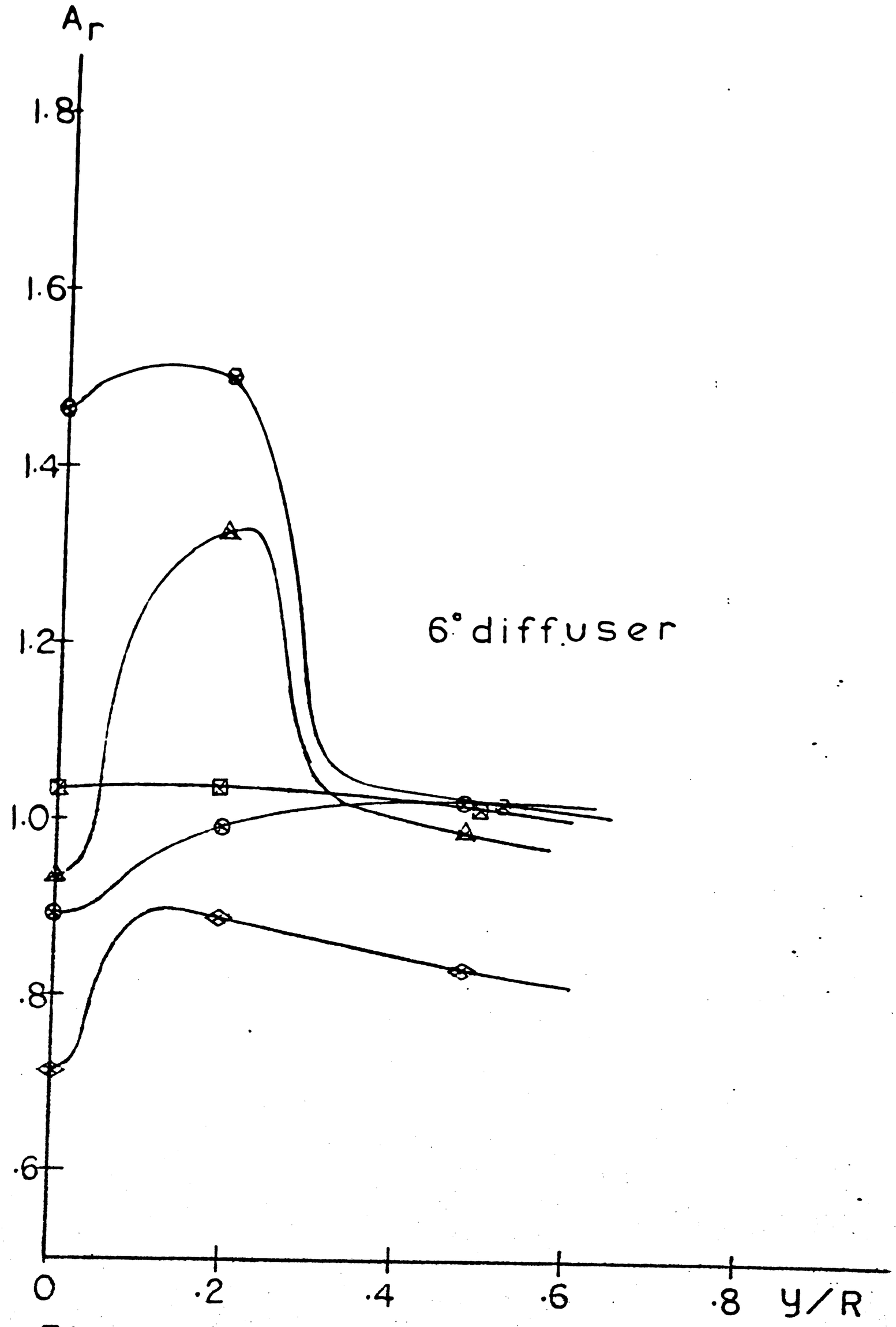

Figure 18 Amplitude Ratios at X-3

Key to symbols in Table 2

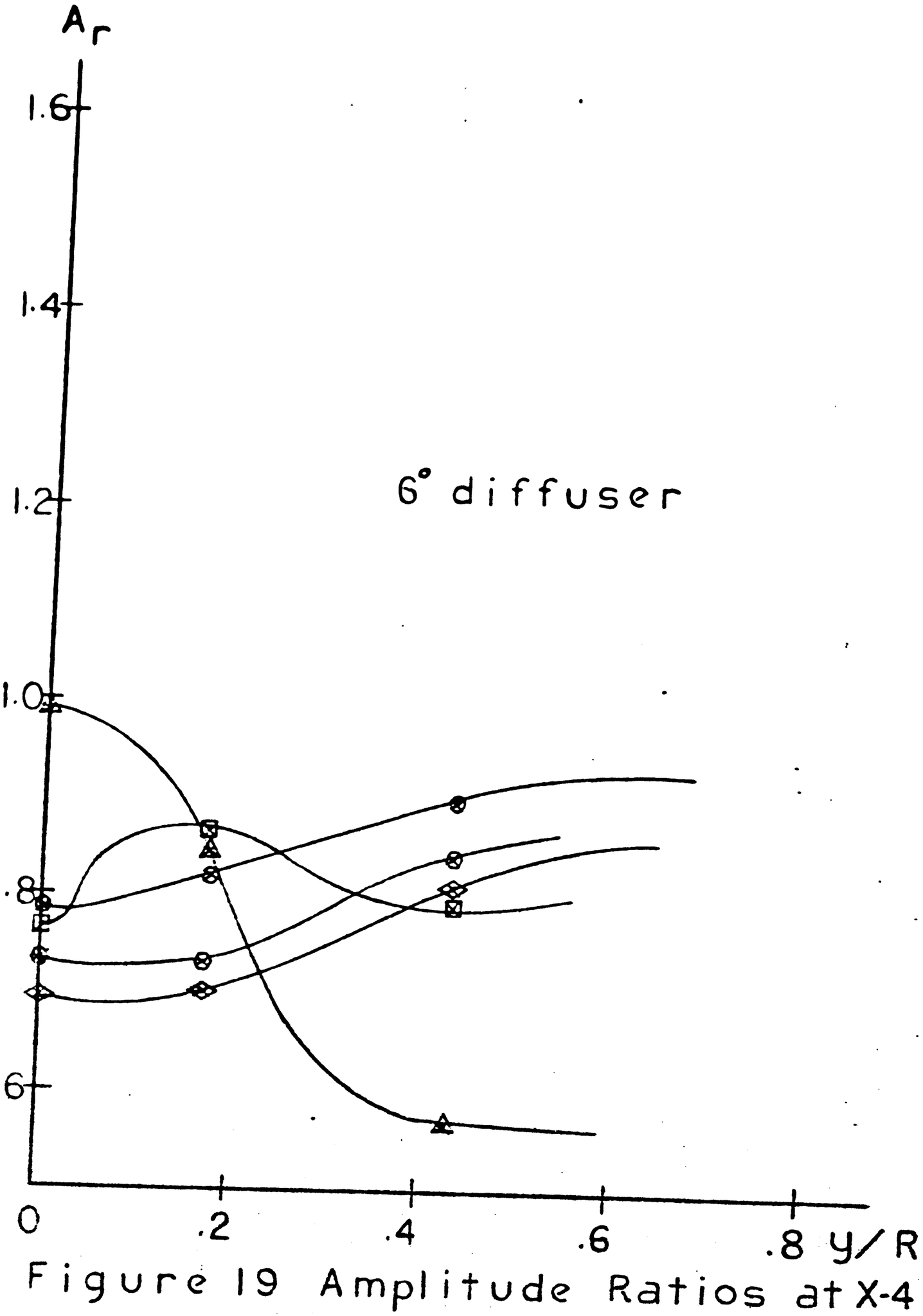

Figure 19 Amplitude Ratios at X-4

Key to symbols in Table 2

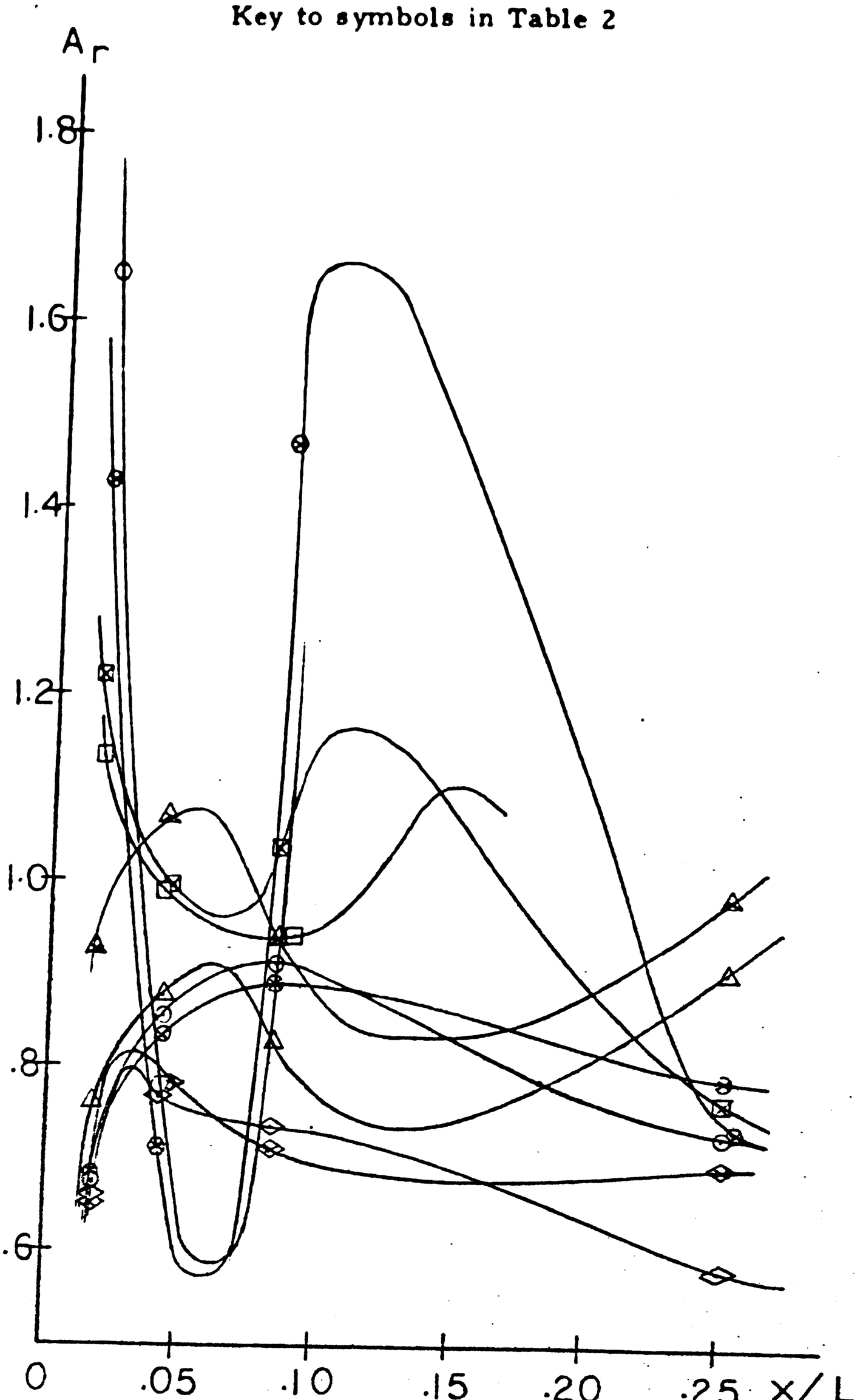

Figure 20 Centerline Ampl. Ratios

Key to symbols in Table 2

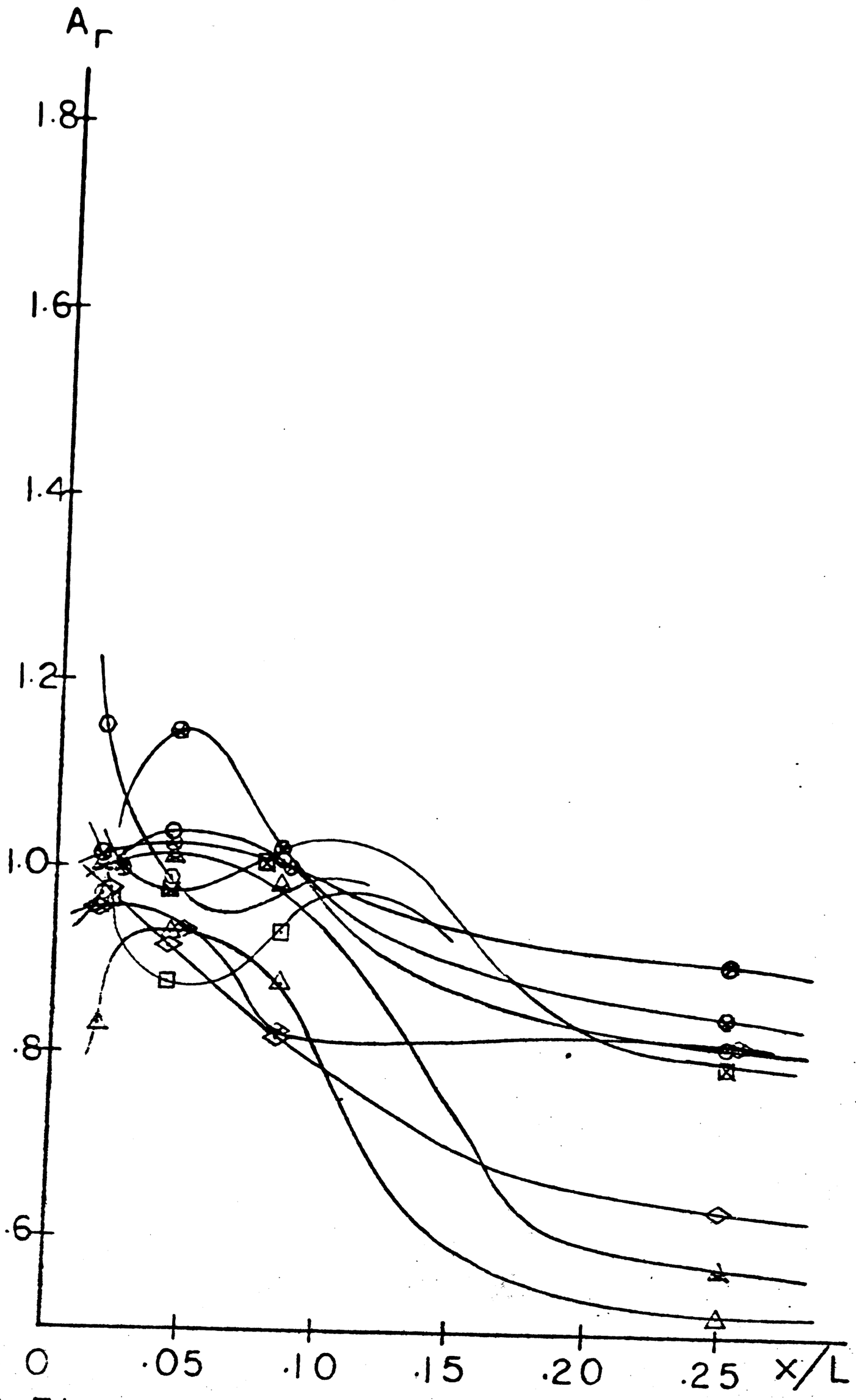

Figure 21 Free Stream Ampl. Ratios

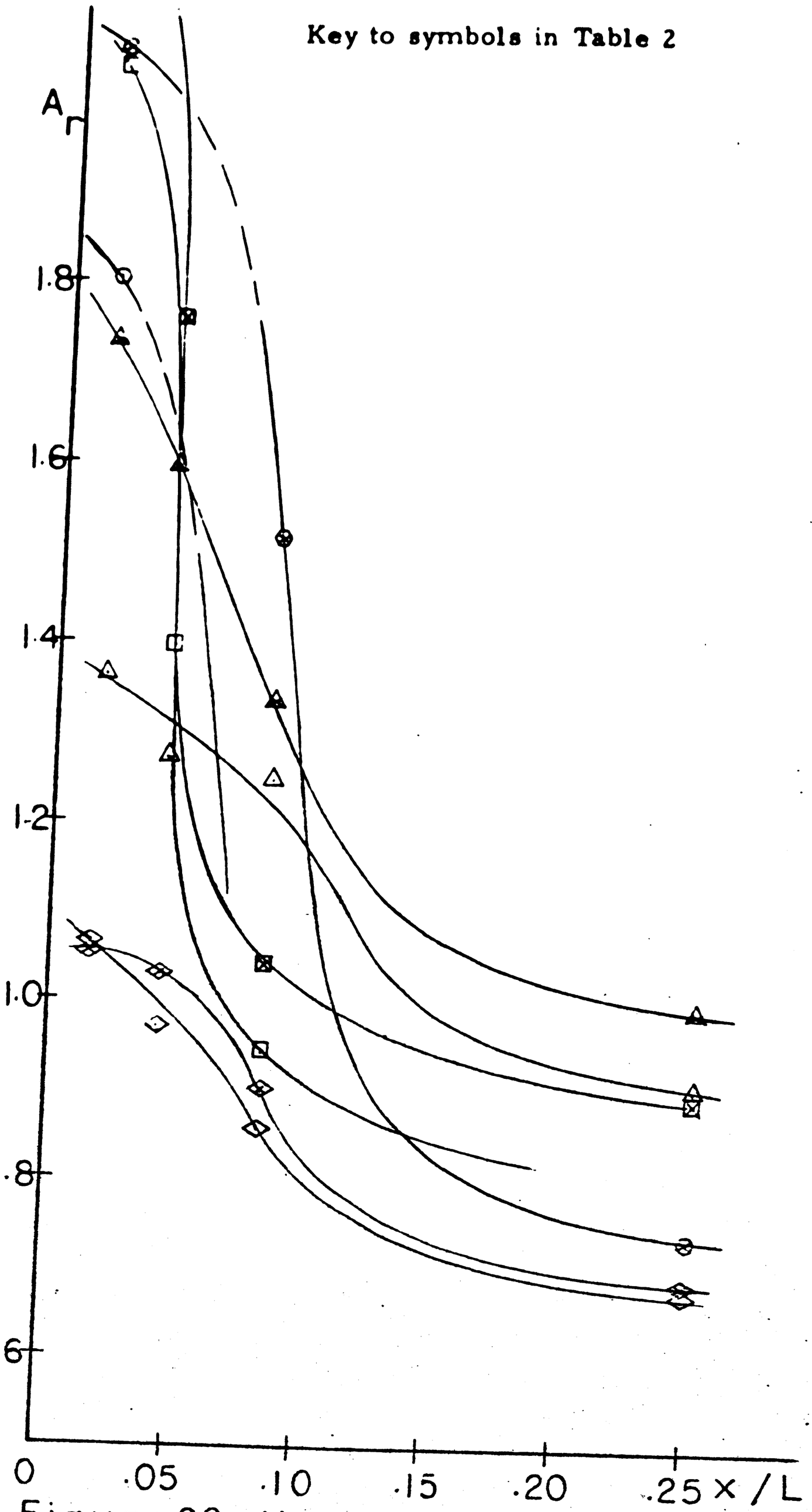

Figure 22 Max Amplitude Ratios

Key to symbols in Table 2

Key to symbols in Table 2

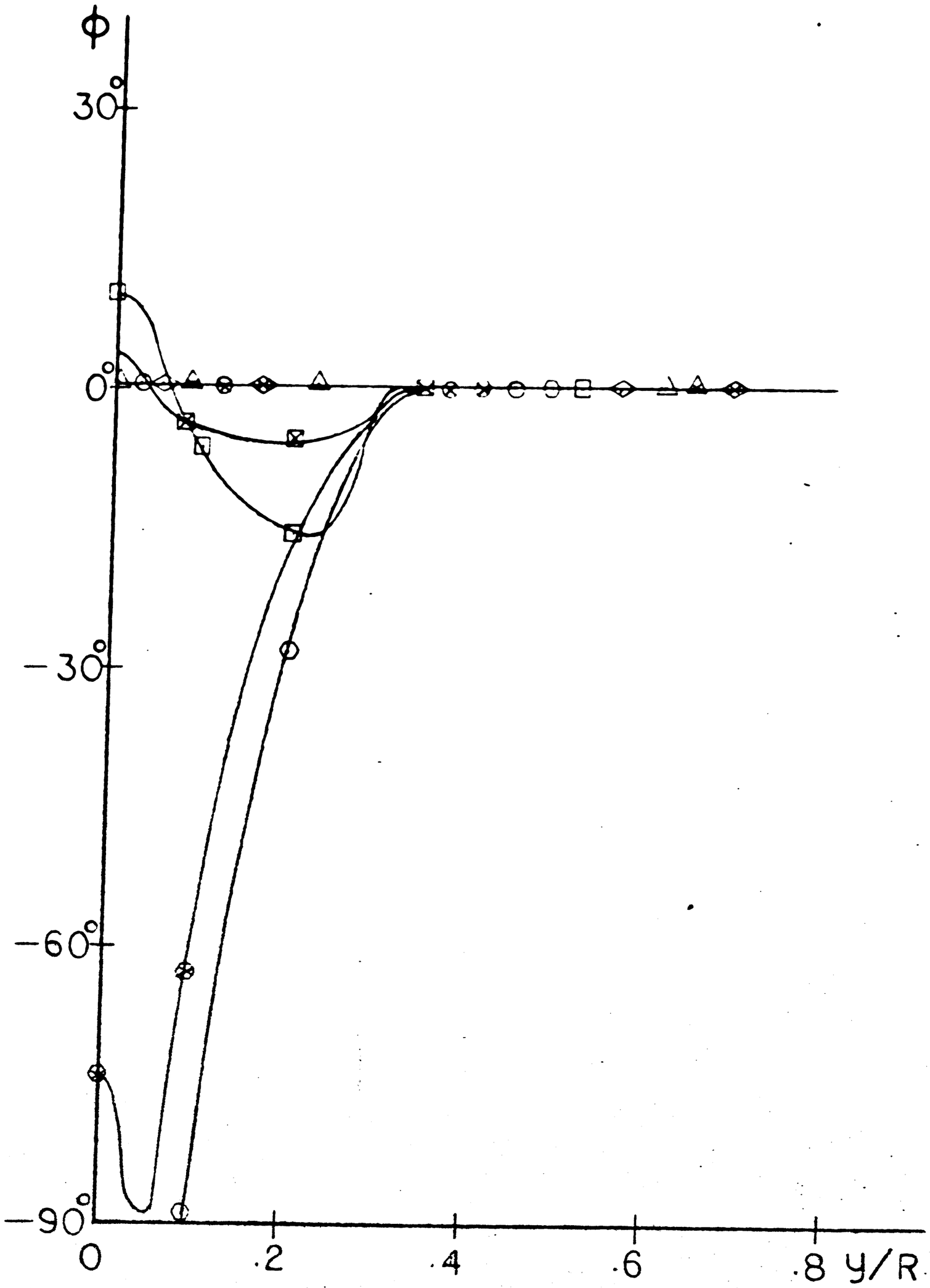

Figure 23 Phase Relations at X-1

Key to symbols in Table 2

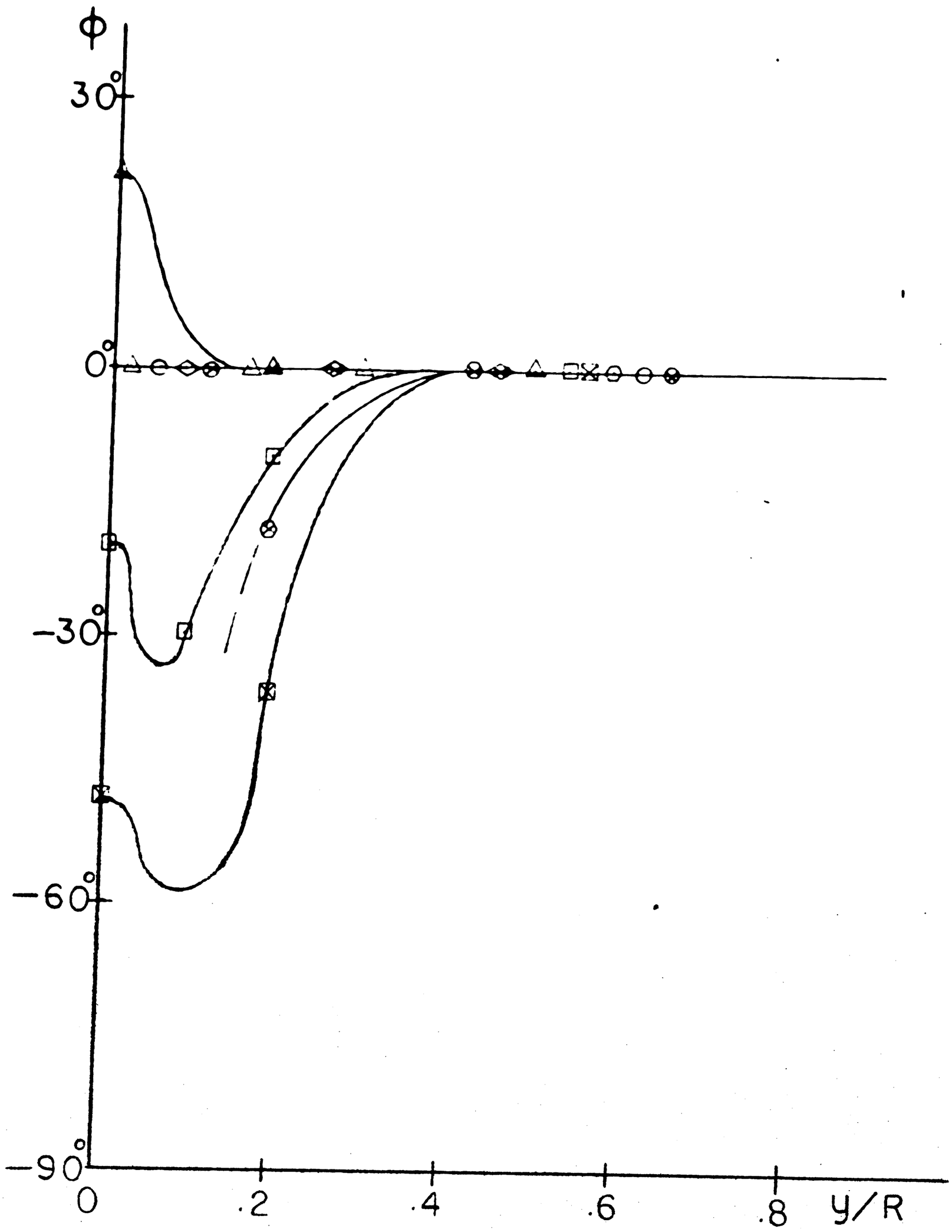

Figure 24 Phase Relations at X-2

Key to symbols in Table 2

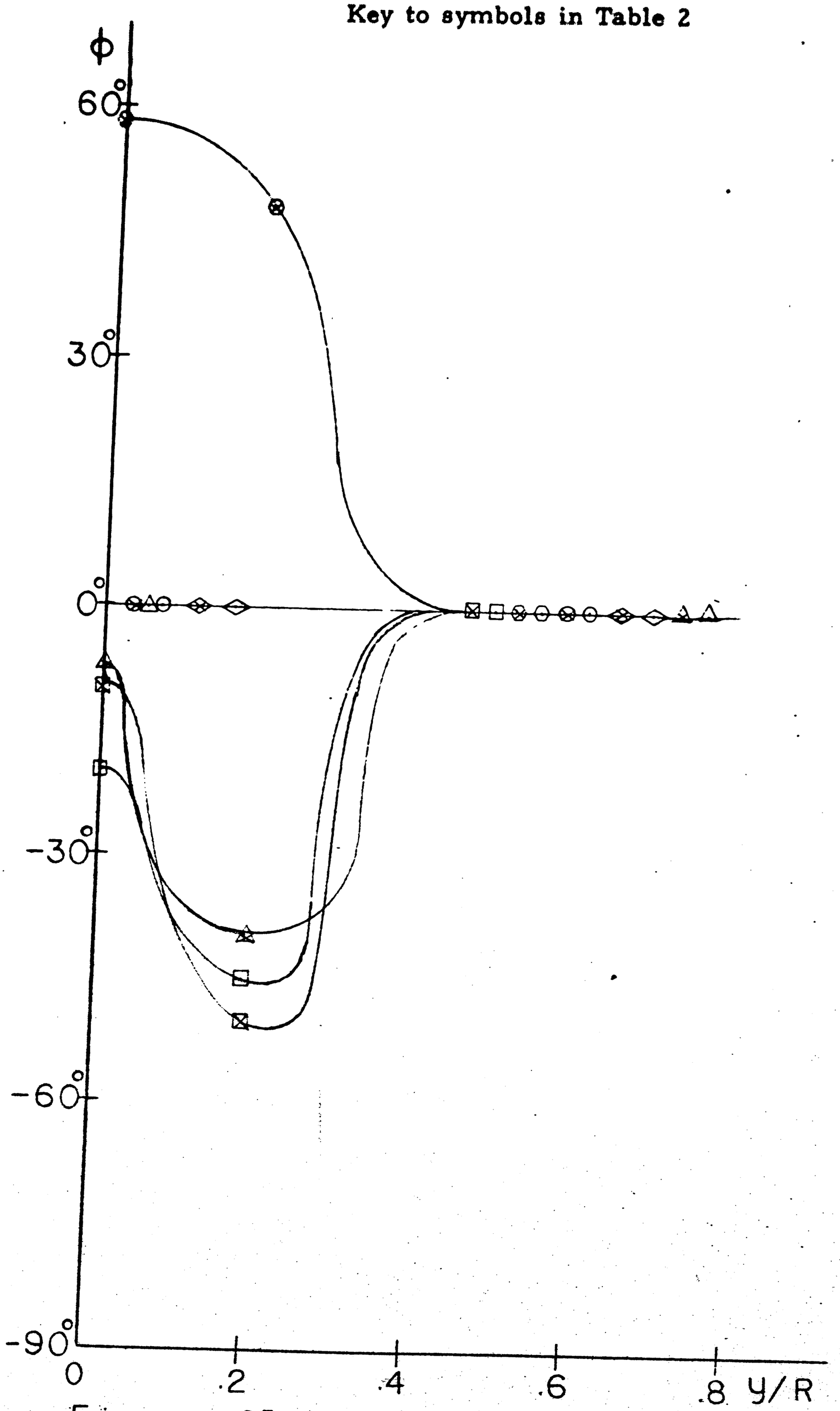

Figure 25 Phase Relations at X-3

Key to symbols in Table 2

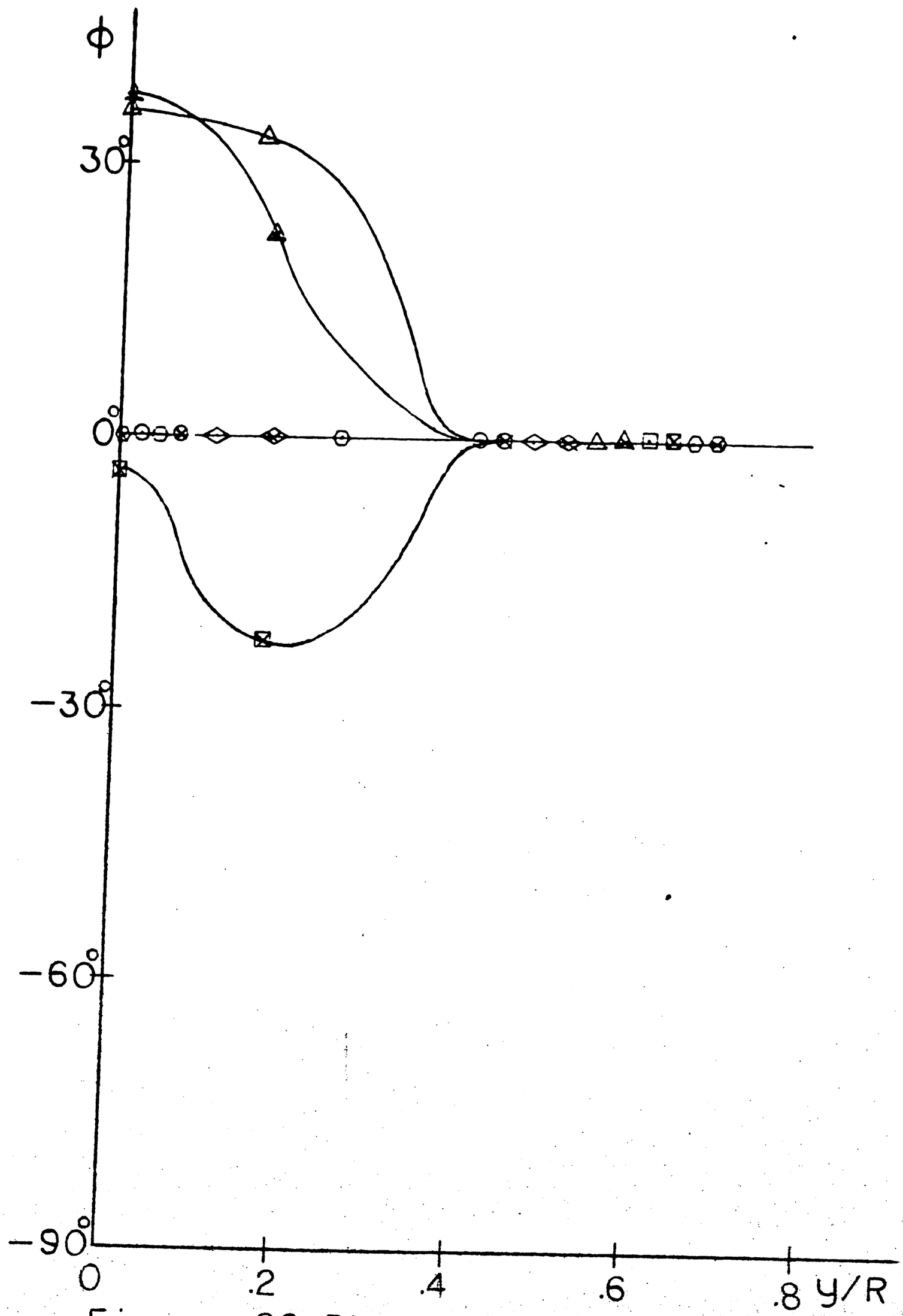

Figure 26 Phase Relations at X-4

LIST OF REFERENCES

1. Chiang, T. et al, "Analysis of Pulsating Flows in Infinite and Finite Conical Nozzles", Journal of Applied Mechanics, Trans. ASME, Series E, Vol. 36, No. 2, June 1969, pp. 159-170.

2. Hill, P. G. and Stenning, A. H., "Laminar Boundary Layers in Oscillating Flows", Journal of Basic Engineering, Trans. ASME, Series D, Vol. 82, No. 3, Sept. 1960, pp. 593-608.

3. Karlsson, S. K. F., "An Unsteady Turbulent Boundary Layer", Journal of Fluid Mechanics, Vol. 5, Part 2, May 1959, pp. 622-636.

4. Lin, C. C., "Motion in the Boundary Layer with Rapidly Oscillating External Flow", Proceedings 9th Intern. Congress of Applied Mechanics, Brussels, 1957, Vol. 4, pp. 155-167.

5. McDonald, M. and Shamroth, S. J., "An Analysis and Application of the Time-Dependent Turbulent Boundary Layer Equations", AIAA Journal, Vol. 9, No. 8, Aug. 1971, pp. 1553-1560.

6. Schachenmann, A. A., "Oscillating Turbulent Flow in a Concial Diffuser", PhD Thesis, Lehigh Univ., Dept. of M. E. and Mechanics, 1974.

7. Schlichting, H., "Boundary-Layer Theory", McGraw-Hill Co., N. Y., Sixth Edition, 1968.

8. Stenning, A. H., and Schachenmann, A. A., "Oscillatory Flow Phenomena in Diffusers at Low Reynolds Number", Journal of Fluids Engineering, Trans. ASME, June 1973.

9. Lab 8/e Software System User's Manual, DEC-8E ALUMA-A-D, DEC, Maynard, Mass., 1972, pp. 1-43.

VITA

I was born on January 13th, 1945 in Varazze, a town near Genova, Italy. My father is Alberto Pittaluga, a former whole-dealer, my mother was Emilia Pittaluga. I visited primary schools in Varazze and secondary schools in Savona, Italy. In 1963 I began my studies in mechanical engineering at the University of Genova where I graduated in 1969 with a degree in mechanical engineering (Laurea in Ingegneria Meccanica). After graduation, I was employed as an engineer in the turbine manufacturing company Ansaldo Meccanico Nucleare of Genova. In 1971 I left this firm to become assistant professor at the University of Genova, Turbomachinery Institute. In July 1973 I came to the U.S.A. to start graduate work at Lehigh University where I am presently.